HHS Public Access

Author manuscript

Clin Radiol. Author manuscript; available in PMC 2017 August 01.

Published in final edited form as:

Clin Radiol. 2016 August ; 71(8): 779–795. doi:10.1016/j.crad.2016.01.011.

Advanced flow MRI: emerging techniques and applications

M. Markl[1,2], **S. Schnell**[1], **C. Wu**[1,2], **E. Bollache**[1], **K. Jarvis**[1,2], **A. J. Barker**[1], **J. D. Robinson**[3,4], and **C. K. Rigsby**[1,5]

[1]Department of Radiology, Feinberg School of Medicine, Northwestern University, Chicago, IL, USA

[2]Department Biomedical Engineering, McCormick School of Engineering, Northwestern University, Evanston, IL, USA

[3]Department of Pediatrics, Division of Pediatric Cardiology, Ann & Robert H Lurie Children's Hospital of Chicago, Chicago, IL, USA

[4]Department of Pediatrics, Northwestern University Feinberg School of Medicine, Chicago, IL, USA

[5]Department of Medical Imaging, Ann & Robert H Lurie Children's Hospital of Chicago, Chicago, IL, USA

Abstract

Magnetic resonance imaging (MRI) techniques provide non-invasive and non-ionising methods for the highly accurate anatomical depiction of the heart and vessels throughout the cardiac cycle. In addition, the intrinsic sensitivity of MRI to motion offers the unique ability to acquire spatially registered blood flow simultaneously with the morphological data, within a single measurement. In clinical routine, flow MRI is typically accomplished using methods that resolve two spatial dimensions in individual planes and encode the time-resolved velocity in one principal direction, typically oriented perpendicular to the two-dimensional (2D) section. This review describes recently developed advanced MRI flow techniques, which allow for more comprehensive evaluation of blood flow characteristics, such as real-time flow imaging, 2D multiple-venc phase contrast MRI, four-dimensional (4D) flow MRI, quantification of complex haemodynamic properties, and highly accelerated flow imaging. Emerging techniques and novel applications are explored. In addition, applications of these new techniques for the improved evaluation of cardiovascular (aorta, pulmonary arteries, congenital heart disease, atrial fibrillation, coronary arteries) as well as cerebrovascular disease (intra-cranial arteries and veins) are presented.

*Guarantor and correspondent: M. Markl, Department of Radiology, Northwestern University, 737 N. Michigan Avenue Suite 1600, Chicago, Illinois 60611, USA. Tel.: +1 312-695-1799; fax: +1 312-926-5991. mmarkl@northwestern.edu.

INTRODUCTION

Cardiovascular function is characterised by the highly integrated and synergistic coupling between the atrial, ventricular, and vascular compartments. The understanding of each individual component has substantially progressed from the molecular to the organ level; however, the direct *in-vivo* assessment of blood flow, which connects all compartments and plays an important role in the development of cardiovascular disease, remains challenging. Specifically, current imaging techniques are limited with respect to the assessment of certain features of blood flow, which is crucial for the comprehensive characterisation of cardiovascular haemodynamics, such as complex changes in three-dimensional (3D) blood flow patterns, pulsatile nature of arterial flow, flow beat-to-beat variability, blood pressure estimation, and flow quantification in small vessels.

Magnetic resonance imaging (MRI) techniques provide non-invasive and non-ionising methods for the accurate anatomical depiction of the heart and vessels throughout the cardiac cycle. In addition, the intrinsic sensitivity of MRI to motion offers the unique ability to acquire spatially registered blood flow simultaneously with morphological data within a single measurement[1-4]. The characterisation of the dynamic components of blood flow with MRI has achieved considerable progress in recent years, in regards to new methodological advances for data acquisition, reconstruction, and analysis. These developments directly impact the ability to assess cardiac and vascular haemodynamics and have opened up new application areas for advanced flow imaging, as summarised in Fig. 1.

RECENT METHODOLOGICAL ADVANCES AND DEVELOPMENTS

Flow imaging with MRI is based on the phase contrast (PC) technique, which can be employed to encode blood flow velocities along all principal dimensions and enables the acquisition of spatially registered information on blood flow simultaneously with morphological data within a single MRI measurement[5]. In current clinical routine practice, PC-MRI is typically accomplished using methods that resolve two spatial dimensions (2D) in individual sections and encode just the time-resolved component of velocity directed perpendicularly to the 2D section. This approach allows measurements of forward, regurgitant, and shunt flows in congenital and acquired heart disease. A number of more advanced and promising flow MRI techniques have been reported, which allow a more comprehensive evaluation of blood flow characteristics, e.g. real-time 2D PC-MRI for the evaluation of flow changes on short timescales and assessment of beat-to-beat variations[6-12]; multiple-venc PC-MRI for the enhancement of the velocity dynamic range and/or encoding of flow velocities as a separate dimension along with assessment of sub-voxel velocity distributions[13,14]; four-dimensional (4D) flow MRI for the comprehensive analysis of complex time-resolved 3D and three-directional blood flow characteristics[15-20]; advanced data analysis and application of fluid dynamics concepts for the quantification of complex haemodynamic properties[21-28,29-41]; multi-dimensional data undersampling and advanced respiratory control for highly accelerated 2D and 4D flow MRI [42-51].

In this article, we will review the status of these MRI techniques and explore emerging techniques and novel applications for the improved assessment of blood flow and

characterisation of cardiovascular disease throughout the human body. We will focus on a select number of applications for the improved evaluation of cardiovascular (aorta, pulmonary arteries, congenital heart disease [CHD], atrial fibrillation [AF], coronary arteries) as well as cerebrovascular disease (intra-cranial arteries and veins). A comprehensive review of the many more applications of advanced flow imaging in the setting of different neurovascular and cardiovascular diseases, however, is beyond the scope of this article and the readers are referred to the literature.

FROM 2D TO 4D

Unlike echocardiography (ECG), the assessment of blood flow in the cardiovascular system with PC-MRI is not limited by acoustic window or probe angle. Traditionally, quantitative blood flow assessment based on ECG-gated time-resolved (cine) 2D PCMRI techniques can include such parameters as peak velocity, retrograde flow (or regurgitant fraction), stroke volume, and shunt volumes (QP/QS). Further indices can also be derived from velocity data, such as pressure gradient through the modified Bernoulli equation to assess, for example, valvular function or aortic coarctation severity.

For routinely used 2D cine PC-MRI, the blood flow velocity is typically encoded in one direction through a 2D section[5,52]; however, placement of the acquisition plane remains challenging and can lead to the underestimation of peak velocities if misplaced or not orthogonal to the flow of interest. This is a common occurrence in cases involving complex flow and where changes in flow direction occur throughout the cardiac cycle, such as with valvular stenosis, valvular regurgitation, or complex CHD. These underestimations can be improved by taking into account all flow directions, which is achieved by three-directional encoding of all three principal velocity directions inside a section of interest [53]. Alternatively, 4D flow MRI (3D cine PC-MRI with three-directional velocity encoding) enables post-hoc time-resolved three-dimensional visualisation and retrospective quantification of blood flow at any location in a 3D volume [15-20] (Fig. 2).

Several studies have investigated the comparison of haemodynamic indices estimated using 4D flow MRI compared to standard 2D velocity-encoded PC sequences [21,54-70], and generally found that aortic and pulmonary flow and velocity indices were significantly underestimated when encoding only one rather than three velocity components (see Fig. 3). On the other hand, good agreement was found between three-directional velocity-encoded sequences, either through a 2D section or in a 3D volume based on 4D flow MRI. These results suggest the importance of three-directional encoding of velocity for estimation of haemodynamic indices, especially when considering quantification of peak velocity or the integrated flow volume; however, integrating PC-MRI with three-directional velocity encoding in routine clinical protocols remains challenging due to increased scan time (acquisition of additional data for velocity encoding along all three dimensions), and thus inability to perform data acquisition in short time and/or during breath-holding. In this context, recent and ongoing developments in sparse sampling techniques, e.g., compressed sensing[42] or radial acquisition[43], as well as multidimensional parallel imaging, e.g., k-t GRAPPA[44-46] (generalised autocalibrating partially parallel acquisitions, Siemens), have shown great potential to accelerate data acquisition and shorten overall scan time.

Alternatively, respiratory gating can be applied to acquire PC-MRI data during free breathing and minimise respiration artefacts. Most widely available approaches include bellows reading or navigator gating[71-74]. A drawback of navigator gating relates to the time it takes to acquire navigator data, which only permits a single or two navigators per cardiac cycle in most situations, often leading to poor prediction of respiratory motion[74]. In addition, detection of motion of the organ of interest is typically based on measurements of remote anatomy (e.g., diaphragm). To address these shortcomings, respiratory self-gating methods have been developed [75,76,77], which repetitively acquire a subset of data of the organ itself to estimate respiratory motion[66,78]. In this context, radial imaging methods offer an elegant approach to inherently acquire motion-related information without time penalty [78,79]. As respiratory gating leads to partial rejection of data acquired during rapid motion, overall scan efficiency is typically reduced by 20–60%, leading to long overall measurement times. As an alternative, advanced retrospective motion correction techniques have been developed that permit correction of the acquired data given an estimate of the underlying motion [80,81].

Methodological improvements based on k-t parallel imaging or compressed sensing have enabled the acquisition of 2D PC-MRI with three-directional velocity encoding during a single breath hold[82]. Their combination with advanced respiration control allowed the acquisition of cardiovascular 4D flow MRI data within clinically acceptable scan times of the order of 5–15 minutes. Continued developments based on alterative data sampling strategies such as radial or spiral data readout have high potential to further reduce scan times. For example, a recent study showed that the combination of highly efficient spiral sampling with dynamic compressed sensing can achieve major acceleration for 4D flow MRI, which allowed the comprehensive assessment of abdominal 4D haemodynamics in a single breath-hold[83].

The increased complexity of PC-MRI data with three-directional encoding and/or volumetric coverage (4D flow) offers the opportunity to obtain more comprehensive and improved information on complex changes of blood flow in cardiovascular disease, compared to standard 2D techniques or echocardiography. A number of investigators have exploited these advantages of multi-dimensional flow imaging to derive new physiological and pathophysiological haemodynamic parameters, such as wall shear stress (WSS) vectors[21,22,84-89], pulse wave velocity (PWV)[29,30], 3D pressure difference maps[25,26,28,90-92], or energy loss[13,31,32,93]. These advanced haemodynamic measures can provide quantitative information on the impact of vascular disease on aortic or pulmonary blood flow patterns.

APPLICATIONS

Aortic and pulmonary disease

It is important to note that flow imaging is typically performed as part of a standard-of-care aortic/pulmonary imaging protocol, which includes additional MRI techniques for the assessment of cardiac function and wall motion (cine imaging), aortic and pulmonary dimensions and geometry (MR angiography), as well as aortic and pulmonary valve morphology and dynamics (cine imaging). The combination with advanced flow imaging provides a comprehensive assessment of aortic/pulmonary structure and function, which has

the potential to contribute to the clinical evaluation of many diseases, such as aortic and pulmonary stenosis (peak systolic velocity) and insufficiency (regurgitant fraction)[94]; aortic aneurysm and/or congenital abnormalities such as bicuspid aortic valve (BAV) or Marfan's syndrome (outflow patterns, peak velocity, wall shear forces)[95]; aortic dissection (fenestration regions, flow in true and false lumen)[96]; aortic coarctation (peak flow velocity, longitudinal post-repair changes)[97]; pulmonary hypertension (PH; altered flow patterns, pressure estimation)[98,99]; and pulmonary branch stenosis (peak velocities, post-stenotic flow patterns).[100]

In addition to improvements in imaging methodology, substantial improvements have been made in the analysis of aortic and pulmonary flow data. Emerging applications include post-processing developments for the quantification of effective orifice area[101,102], aortic stiffness-related PWV [103,104], pressure difference maps [97], and WSS[21,22,105-109]. Modified strategies have also made efforts to use valve tracking to improve the ability to quantify stroke volume and retrograde fraction across the heart valves [110,111].

Applications of flow imaging in the thoracic aorta have provided evidence that aortic valve disease such as the frequently occurring congenital BAV (affecting 1–2% of the general population[112-115]) can result in significant, valve-mediated changes in aortic flow patterns. 4D flow MRI studies have shown that valve abnormalities can be associated with complex flow disturbances, such as altered systolic jet flow patterns (see Fig. 4) and elevated WSS in the aorta[86,95,106,116-120]. WSS is a known stimulus for arterial mechanotransduction, which can impact endothelial cell function and result in vascular remodelling (e.g., dilation). A recent study[95] demonstrated that altered aortic haemodynamics can be considered as a physiological mechanism by which valve morphology can influence the phenotypic expression of aortopathy. A subsequent study in BAV patients that included both *in-vivo* 4D flow MRI and aortic tissue resection in patients undergoing aortic repair provides strong support for this pathomechanism[105]. Correlation of aortic haemodynamics with histopathology of the resected aortic tissue showed that regionally elevated WSS patterns were closely associated with abnormal aortic tissue architecture, biomechanics, and protein expression.

Other promising applications of aortic 4D flow MRI are related to atherosclerosis and complex aortic plaques (thickness ≥4 mm), which act as potential sources for embolic stroke. Complex plaques in the descending aorta, where they occur most frequently[121], were traditionally not considered a source of stroke as embolisation would require diastolic reverse (upward) flows from the DAo plaque into the brain supplying supra-aortic vessels to establish a mechanism[122,123]. Recent 4D flow MRI studies have shown that marked diastolic flow reversal in the DAo is frequently found in patients with aortic atherosclerosis, even in the absence of aortic valve insufficiency[124-126]. In fact, there is strong evidence that descending aorta plaques can be sources of embolic stroke via retrograde embolisation. In a study of 94 acute stroke patients, 4D flow MRI was employed for the *in-vivo* evaluation of aortic 3D blood flow characteristics[127]. In more than 55% of patients, 3D blood flow visualisation revealed reverse flow from descending aorta plaques into the supraaortic arteries supplying the cerebrovascular territory affected by stroke as a possible mechanism for retrograde cerebral embolisation.

In the pulmonary system, flow imaging has been employed to assess WSS [128,129] and flow vorticity [130] in the presence of PH. Reiter *et al.*[131] used time-resolved 3D velocity information to visualise this flow anomaly and found an unusual flow structure in the main pulmonary artery (MPA) of PH patients[131]. A vortex in the primary flow direction of the MPA formed below the right pulmonary artery (RPA). Thus, the time persistence of this vortex was found to be correlated with the degree of hypertension as measured by mean pulmonary artery pressure. Visualisation of complex flow patterns in the pulmonary arteries may thus have the potential to provide a noninvasive vortex-based diagnosis of PH.

Complex CHD

The most common congenital disorder, CHD occurs in an estimated nine per 1000 live births worldwide[132,133]. CHD can be associated with complex alterations of cardiovascular physiology and flow (e.g., hypoplastic heart) and surgical correction or palliation of the defect are often necessary (e.g., Fontan procedure). As a result, a comprehensive assessment and monitoring of longitudinal changes in cardiovascular physiology from birth to adulthood are critical in these patients. Current diagnostic tools, however, are limited by invasiveness (catheter angiography) or provide an incomplete assessment of the often complex haemodynamics in patients with CHD[134,135].

Although techniques such as echocardiography or CT can provide anatomical or flow information, only MRI is capable of providing non-invasive assessment of haemodynamics, cardiac function, and cardiovascular anatomy within a single examinatino[136-139]; however, flow MRI in this patient population is challenging and requires time-consuming and operator-dependent placement of multiple imaging sections to study multiple vessels, which can result in misalignment with respect to the flow direction and thus underestimation of velocity[140]. The situation is exacerbated in paediatric CHD by small vessel size, high heart rates, and limited ability to perform long/multiple breath holds. As a result, MRI-based evaluation of CHD can require long total examination times (60–90 minutes) and is often performed during general anaesthesia in children under the age of 6–8 years [141,142]. These challenges drive the need for flow imaging with high spatial and temporal resolution, short imaging times, and full coverage of complex cardiovascular malformations [143-145].

Advances in MRI hardware such as high-field MRI systems >1.5 T for improved signal-to-noise ratio (SNR) and spatial resolution; improved gradient performance for faster sequences; and high sensitivity multi-channel receiver coils, enabling parallel imaging with high acceleration factors have led to promising new applications for flow imaging in patients with CHD. Specifically, highly accelerated imaging with spatio-temporal undersampling and compressed sensing/parallel imaging reconstruction in combination with compensation for respiratory motion (e.g., self-navigator gating or image registration) can be employed to assess flow with greater flexibility (spatial, temporal resolution) and with short scan times. An emerging and promising technique is real-time flow imaging in CHD[146-148], which can greatly simplify flow imaging by data acquisition during free breathing and without the need for ECG gating. In addition, the technique is well suited to assess important respirophasic effects on flow (e.g., changes in venous flow in the Fontan circulation during inspiration versus expiration), which cannot easily be assessed with standard 2D PC flow methods.

Whole-heart 4D flow MRI techniques allow for a non-invasive comprehensive assessment of cardiovascular haemodynamics in the heart and surrounding great vessels (see Fig. 5). Although scan times are still long due to full volumetric coverage of the entire heart (10–15 minutes depending on heart rate and respiration control efficiency), the main advantages of whole-heart imaging are that it facilitates the systematic assessment of blood flow in multiple vessels and enables the retrospective analysis of any region of interest within the imaging volume. Previous studies have shown that the technique can reliably identify altered 3D flow characteristics related to the post-interventional status in patients with CHD [149-152]. In addition, 4D flow MRI based flow quantification has been shown to be equivalent or even improved when compared to 2D techniques, while needing less imaging time than the positioning of multiple planes[58,61,64,67,68]. More recent developments combining parallel imaging or compressed sensing with 4D flow MRI have high potential to reduce scan times to <5 minutes.

AF

AF affects 33.5 million patients worldwide. The most serious complication, stroke, is generally attributed to embolism of thrombus from the left atrium (LA); however, current clinical risk scores (e.g., CHA_2DS_2-VASc) have limited predictive accuracy, as they are based on upstream clinical factors (age, gender, diabetes, etc.) rather than individual physiological factors implicated in LA thrombus formation.

Studies utilising transoesophageal echocardiography (TOE) have shown that decreased flow in the LA and particularly in the LA appendage (LAA), which is the typical site of thrombus formation, is an independent risk factor for stroke in AF;[153-155] however, TOE requires oesophageal intubation, and is thus an impractical approach as a screening tool in the population. Furthermore, due to inherent technical limitations, TOE cannot fully assess the complex 3D patterns of flow and stasis in the LA and LAA, and does not provide detailed information on LA and LAA 3D shape and geometry. 4D flow MRI can overcome limitations of TOE by providing the ability to measure complex 3D blood flow patterns *in vivo*. A number of studies have shown that 4D flow MRI could be a promising tool for the comprehensive assessment of atrial haemodynamics.[156-158]

As illustrated in Fig. 6, atrial 4D flow MRI can be employed for the non-invasive *invivo* assessment of atrial flow dynamics with full spatial (3D) and temporal (cardiac cycle) coverage of the atrium. After 3D segmentation of the LA, anatomical maps of left atrial flow dynamics (mean velocity, peak velocity stasis) can provide intuitive visualisation of atrial flow dynamics (Fig. 6b). Specifically, LA and LAA maps of the relative amount of flow stasis (i.e. fraction [%] of LA or LAA with velocities below a certain threshold) can visualise regions exposed to high stasis or reduced velocities and thus potentially heightened risk for thrombogenesis.

A number of pilot feasibility studies have demonstrated the potential of atrial 4D flow MRI and derived maps of LA flow dynamics to detect changes in global and regional LA flow dynamics associated with AF, age, and LA volume[158-160]. 4D flow MRI detected significant changes in LA haemodynamics and reduced LA velocities in patients with a history of AF, compared to young and age appropriate control groups. Moreover, reduction in LA

velocities was significantly associated with the standard-of-care clinical CHA_2DS_2-VASc risk score.

It is important to recognise that 4D flow MRI data are acquired over multiple heartbeats and the resulting images represent a composite of blood flow over the entire acquisition time. As a result, beat-to-beat flow variations in AF patients with cardiac arrhythmia cannot be captured by this technique. A systematic analysis of the impact of beat-to-beat variations on LA flow characteristics is thus not possible, particularly in the presence of arrhythmia. Recent advances in MRI data acquisition strategies allow for real-time assessment of beat-to-beat variation in the presence of AF and breathing exercises (such as the Valsalva and Mueller manoeuvres) [8,161,162]. To achieve sufficiently high frame rates needed for real-time flow acquisitions, optimised and accelerated 2D flow imaging pulse sequences have been developed, which combine effective data readout modules (e.g., echo planar imaging, EPI) with data undersampling and parallel imaging data reconstruction (e.g., compressed sensing, k-t-acceleration in spatial and temporal dimension). In addition, shared velocity encoding[10,163] has been proposed to further improve temporal resolution and is based on the concept of sharing sets of full k-space data between adjacent time frames in order to double the effective frame rate. Based on these developments, 2D real-time flow imaging with through-plane velocity encoding can be performed with temporal update rates on the order of 30–50 ms (see Fig. 7).

The combination of metrics of persistent multi-beat flow patterns (4D flow: velocity histograms, stasis) with measures of beat-to-beat flow variations (real-time flow imaging) may have the potential to better understand the impact of AF on LA and LAA haemodynamics and thus thromboembolic risk.

Coronary artery flow

A non-invasive technique for measuring coronary flow would be highly desirable in the management of coronary circulatory disorders. For example, exercise testing and invasive catheter angiography are often used to induce coronary microcirculatory hyperaemia, thereby increasing coronary blood by up to fourfold. The ratio of stress versus rest coronary flow (or fraction flow reserve, FFR) can be used to quantify the physiological significance of coronary stenosis.

The major challenge in using MRI for the assessment of flow in coronary arteries includes the need for high spatial resolution, due to their small size. Additionally, coronary flow MRI should resolve and/or provide the ability to follow the tortuous path and highly dynamic cardiac and respiratory induced motion of the coronary arteries during the cardiac cycle. Several studies have addressed these challenges and successfully acquired coronary flow images by using advanced imaging acceleration techniques (see Fig. 8) or more efficient non-Cartesian data sampling strategies, such as spiral trajectories in combination with motion control (e.g., navigator echoes)[164-167]. Reports include the validation of PC-MRI in coronary arteries by assessing flow reserve after stent deployment in comparison with intracoronary Doppler ultrasound [168]. Another study showed good agreement for MRI-derived coronary flow reserve compared to myocardial blood flow obtained by positron-emission tomography (PET) [169]. To date, only few clinical applications have been reported.

Among them, studies include the assessment of myocardial flow reserve in patients with coronary artery disease (CAD) after stent implantation in the proximal left anterior descending artery (LAD) by Saito *et al.*[170]; the comparison of coronary flow during rest versus exercise stress in healthy adults and CAD patients by Hays *et al.*[171]; and profiling of CAD by combining MRI-based assessment of vessel wall remodelling and related myocardial blood flow by Jahnke *et al.*[172].

Although methodologically challenging, comprehensive MRI protocols including coronary flow assessment could provide a promising non-invasive approach for the direct assessment of coronary vessel wall remodelling, and the resultant pathophysiological consequences on the level of epicardial coronary and myocardial blood flow in patients. Further improvements in hardware and imaging at high field strength (3 T and above)[173] are expected to enhance the spatial resolution needed for reliable coronary flow imaging methods. Nevertheless, coronary motion remains a major challenge. As a result, the measurement and quantification of coronary blood flow is easier to perform at the larger and more easily identifiable coronary sinus compared to whole-heart flow quantification. Retrospective motion correction for navigated 2D cine velocity mapping [74] or data acquisition using readout modules less sensitive to motion (radial, spiral) are promising but further developments and studies evaluating the reliable assessment of flow in all coronary segments are warranted. If successful, an emerging application would be the quantification of FFR, which is currently performed invasively (catheter) or using a combination of computed tomography (CT) angiography and computational fluid dynamics (CFD) [174,175]. MRI could provide a valuable non-invasive and radiation free alternative by combining coronary MRA with rest and stress coronary flow imaging.

Cerebrovascular flow

In clinical practice, transcranial Doppler ultrasound is routinely used for cerebrovascular flow measurements; however, the technique is operator-dependent and significantly limited by the available acoustic windows of the head. 2D PC-MRI can provide reliable flow measurements in large intracranial arteries and veins, not limited by location. Challenges for using 2D PC-MRI for flow measurement include small and tortuous vessels[176], complex vascular anatomy, and the need for manual placement of 2D imaging planes in multiple vessel segments. Recent improvements in intracranial flow MRI include automatic positioning of 2D planes for flow quantification based on a previously acquired angiogram [177] or the application of 4D flow MRI, which additionally offers 3D blood flow visualisation and retrospective flow quantification. Emerging applications of cerebrovascular flow imaging include the haemodynamic evaluation of intra-cranial aneurysms, arteriovenous malformations (AVM), and intracranial atherosclerotic disease (ICAD), as well as venous flow.

A large number of studies investigating flow patterns in intracranial aneurysms were based on CFD [109,178-187] techniques in conjunction with subject-specific geometries extracted from medical images [179,184,188,189]. Findings from these studies revealed a wide variety of complex intra-aneurysmal flow patterns that were strongly dependent on patient-specific vascular geometry. As an emerging pattern, a number of studies showed that changes in

WSS along the wall of intracranial aneurysms may be associated with risk of aneurysm growths or rupture[109,190]; however, CFD has limitations, such as assumptions concerning blood properties, boundary conditions, and vessel properties [191179,192]. As an alternative, 4D flow MRI is increasingly used to assess intra-aneurysmal 3D haemodynamics *in vivo*. Several groups have reported the successful measurement and evaluation of intra-aneurysmal flow and WSS in patient feasibility studies [109,185,193-198], indicating the potential of flow MRI to assist in the classification of individual aneurysms pre-intervention.

In patients with cerebral AVMs, the pathological vascularisation (direct shunting of blood from arterial to the venous sides without an intervening capillary bed) leads to abnormal haemodynamics. Flow information is potentially valuable for a better understanding of the impact of a focal AVM on the flow redistribution in the brain and/or in treatment planning by attempting to identify the feeding arteries with highest flow, enabling efficient and targeted embolisation treatment. 2D PC-MRI has been used in a number of studies to quantify flow in pre-defined vessels, such as feeding arteries. Earlier reports demonstrated that flow MRI could successfully be used to visualise and quantify flow and velocity[199], to compare flow velocity in feeding and contralateral vessels and following embolisation treatment[200], and to compare total cerebral arterial inflow (basilar and internal carotid artery flow rates) [201]. More recently, 2D PC-MRI in combination with automated 2D plane placement at multiple anatomical regions was employed to assess haemodynamic changes after AVM embolisation[202]. To date, there are only a few studies investigating the diagnostic value of 4D flow MRI for the assessment of AVM flow characteristics. Recent reports include the quantification of flow and WSS in patients using a highly optimised radial 4D flow technique [203,204]. Additional studies demonstrated the potential of 4D flow MRI for the evaluation of global and regional AVM flow characteristics as illustrated in Fig. 9 [205,206]. The findings showed that 4D flow MRI can assess treatment-induced changes in cerebrovascular flow distribution and were able to demonstrate significant associations between 4D flow metrics, cerebral perfusion indices, and AVM risk factors such as the Spetzler–Martin grade[206].

Intra-cranial atherosclerotic plaques can alter local and global haemodynamics (particularly proximal or distal to stenosed vessels). Currently, intracranial haemodynamic disturbance in patients with ICAD is primarily assessed using Doppler ultrasound. 2D PC-MRI has also been used to classify stenosis severity, predict risk of recurrent stroke, and detect in-stent restenosis after stent placement;[207-210] however, very few studies have been performed to characterise the 3D blood flow disturbance and flow redistribution across the major cerebral arteries in patients with ICAD. An early study by Hope *et al.*[195] reported that TOF MRA overestimated the degree of stenosis and that 4D flow MRI velocity measurements could improve accuracy of diagnosis, when compared to catheter angiography. It should be noted that current flow imaging techniques (2D and 4D) are also limited by insufficient spatial resolution for the characterisation of blood flow at sites of critical or severe stenosis. Instead, post-stenotic flow is typically used to represent the regional flow in the stenotic artery; however, the accuracy of flow quantification in the smaller arteries (e.g., anterior/posterior cerebral arteries) may be compromised by partial volume effects. Higher magnetic field strength (7 T) with increased spatial resolution may be required for improved flow assessment in the smaller vessels.

Cerebral venous blood flow attracts less attention compared to arterial flow, but the venous system is of great importance to the understanding of some cerebrovascular diseases, such as cerebral venous thrombosis or cerebral venous sinus stenosis in patients with intracranial hypertension. The assessment of intra- or extra-cranial venous flow can be particularly challenging as there are several factors that can affect flow measurement [211], such as head and limb position[212], respiration, heart rate, or hydration status. Nevertheless, 2D PC-MRI has been applied to quantify physiological cerebral venous flow[213], for the concomitant analysis of arterial, venous and cerebrospinal fluid flows[211], the assessment of intracranial venous haemodynamics in normal and patients with cerebral venous thrombosis[214], and to evaluate physiological variation in dural venous sinus flow[215]. Volumetric measurement of cerebral venous 3D flow dynamics[216,217] and assessment of cerebrospinal venous flow using radial 4D flow MRI[218] have also been reported.

Limitations of intracranial flow MRI include the spatial resolution and low sensitivity to slow blood flow. For the detailed evaluation of cerebrovascular flow, it would thus be desirable to gain quantitative information on both lower venous and high arterial blood flow velocities, which can differ by one order of magnitude even in normal subjects (10 versus 150 cm/s). Current flow MRI techniques, however, measure blood velocity (v) based on a single user-defined velocity sensitivity (venc), usually set above the expected maximum velocity. This single-venc acquisition can result in either velocity aliasing for unexpected higher blood flow velocities (v>venc) or high noise levels for slow flow (v<<venc). Current MRI protocols thus lack the dynamic range to reliably assess the full velocity spectrum. To improve upon this limitation, several studies have investigated multi-venc approaches based on several flow acquisitions with a set of two or more vencs [219-221]. The resulting high-venc data can then be used for complete anti-aliasing of the low-venc data while maintaining the favourable velocity-to-noise characteristics of the latter. Alternative approaches include five-point balanced flow encoding to reduce noise and aliasing in phase images [222], or varying velocity encoding during systole or diastole [223].

Studies performed at ultra-high field (7 T) have shown that the assessment of smaller calibre-vessels as well as small aneurysms can be improved (e.g., posterior cerebral artery) and their pulsatility index can be measured[173,224,225]. In addition, several advanced acceleration methods for the improvement of spatial resolution and/or reduction of total scan time have been successfully explored including k-t BLAST[226], k-t GRAPPA, k-t SENSE[227], radial[227] and spiral[228] sampling schemes as well as compressed sensing approaches[229,230].

Fig. 10 shows results based on k-t accelerated dual-venc 4D flow MRI at 7 T and illustrates that the combination of the novel developments described above can enable flow imaging with significantly improved dynamic range for the assessment of both low venous and high arterial flow velocities within a single scan.

DISCUSSION AND CONCLUSIONS

In the past decade, substantial advances in flow imaging (including imaging techniques and data analysis) have been made that have led to a number of emerging applications for the improved assessment of cardiovascular and cerebrovascular diseases. The application areas

presented in this review reflect the view of the authors. A comprehensive review of the many more and growing applications of advanced flow imaging in the setting of different neurovascular and cardiovascular diseases, however, was beyond the scope of this article and the readers are referred to the literature.

A number of hurdles and limitations for the more widespread application of the emerging flow imaging techniques presented in this review exist. Eddy currents and phase offsets remain longstanding technical challenges that introduce measurement error across all phase-contrast approaches, including the advanced methods presented here[231]. These errors, which manifest as phase shifts on a regional, global, and temporal basis, will compromise the ability to accurately quantify integrated parameters such as stroke volume[231-234]. A number of studies have investigated various correction approaches[57,234-236]; however, there is no widespread agreement as to a universal correction protocol. The lack of standardised analysis tools for regional flow quantification and analysis of PC data with three-directional velocity encoding and/or 3D volumetric coverage is currently a major hurdle for their more widespread clinical application. In addition, many promising techniques for advanced sparse sampling and timing acceleration have been developed in the past decade; however, current limitations include a wide disparity of techniques used for sparse sampling and imaging acceleration, as well as a lack of standardised quality metrics that define the optimal use of these methods for clinical applications.

To further the availability of these techniques and facilitate their translation into the clinic, workflow efforts towards standardisation across different MRI vendor platforms and data analysis software are warranted. These include fundamental aspects such as the consistent presentation of flow directions in MRI images and the clear definition of data header fields with flow relevant information (e.g., velocity sensitivity) across all platforms. In addition, software solutions should report standardised flow metrics and include quality control to provide the user with feedback regarding phase offset errors and corrections that have been applied to the flow data. To achieve these aims, multicentre studies are necessary to establish the repeatability of various aspects of the technique across centres and identify the most robust and reproducible flow metrics. In addition, further longitudinal studies of emerging novel haemodynamic measures, such as WSS or stasis maps, are needed to evaluate their diagnostic value for patient risk stratification and therapy management.

In summary, flow imaging with MRI has undergone and continues to undergo a substantial transformation, from simple techniques measuring one-directional blood flow velocities at a specific location to a more compressive diagnostic tool that can assess 3D blood flow, quantify real-time beat-to-beat respirophasic changes in flow, or derive advanced metrics of cardio- and cerebrovascular haemodynamics, such as pressure gradients or WSS.

ACKNOWLEDGEMENTS

Grant support was received from the NIH NHLBI grants R01HL115828 and K25HL119608, and American Heart Association fellowships 14PRE18620016 and 14PRE18370014.

REFERENCES

1. Burt CT. NMR measurements and flow. J Nucl Med. 1982; 23(11):1044–1045. [PubMed: 6215469]
2. Nayler GL, Firmin DN, Longmore DB. Blood flow imaging by cine magnetic resonance. J Comput Assist Tomogr. 1986; 10(5):715–722. [PubMed: 3528245]
3. Firmin DN, Nayler GL, Klipstein RH, Underwood SR, Rees RS, Longmore DB. In vivo validation of MR velocity imaging. J Comput Assist Tomogr. 1987; 11(5):751–756. [PubMed: 3655038]
4. Pelc NJ, Herfkens RJ, Shimakawa A, Enzmann DR. Phase contrast cine magnetic resonance imaging. Magn Reson Q. 1991; 7(4):229–254. [PubMed: 1790111]
5. Nayak KS, Nielsen JF, Bernstein MA, et al. Cardiovascular magnetic resonance phase contrast imaging. J Cardiovasc Magn Reson. 2015; 17(1):71. [PubMed: 26254979]
6. Nayak KS, Pauly JM, Kerr AB, Hu BS, Nishimura DG. Real-time color flow MRI. Magn Reson Med. 2000; 43(2):251–258. [PubMed: 10680689]
7. Joseph AA, Merboldt KD, Voit D, et al. Real-time phase-contrast MRI of cardiovascular blood flow using undersampled radial fast low-angle shot and nonlinear inverse reconstruction. NMR Biomed. 2012; 25(7):917–924. [PubMed: 22180216]
8. Untenberger M, Tan Z, Voit D, et al. Advances in real-time phase-contrast flow MRI using asymmetric radial gradient echoes. Magn Reson Med. Jun 22.2015 [Epub ahead of print]. doi: 10.1002/mrm.25696
9. Fasshauer M, Joseph AA, Kowallick JT, et al. Real-time phase-contrast flow MRI of haemodynamic changes in the ascending aorta and superior vena cava during Mueller manoeuvre. Clin Radiol. 2014; 69(10):1066–1071. [PubMed: 25060931]
10. Lin HY, Bender JA, Ding Y, et al. Shared velocity encoding: a method to improve the temporal resolution of phase-contrast velocity measurements. Magn Reson Med. 2012; 68(3):703–710. [PubMed: 22139889]
11. Steeden JA, Atkinson D, Taylor AM, Muthurangu V. Assessing vascular response to exercise using a combination of real-time spiral phase contrast MR and noninvasive blood pressure measurements. J Magn Reson Imaging. 2010; 31(4):997–1003. [PubMed: 20373446]
12. Nezafat R, Kellman P, Derbyshire J, McVeigh E. Real time high spatial-temporal resolution flow imaging with spiral MRI using auto-calibrated SENSE. Conf Proc IEEE Eng Med Biol Soc. 2004; 3:1914–1917. [PubMed: 17272087]
13. Binter C, Knobloch V, Manka R, Sigfridsson A, Kozerke S. Bayesian multipoint velocity encoding for concurrent flow and turbulence mapping. Magn Reson Med. 2013; 69(5):1337–1345. [PubMed: 22700280]
14. Macgowan CK, Liu GK, van Amerom JF, Sussman MS, Wright GA. Self-gated Fourier velocity encoding. Magn Reson Imaging. 2010; 28(1):95–102. [PubMed: 19553052]
15. Ebbers T. Flow imaging: cardiac applications of 3D cine phase-contrast MRI. Curr Cardiovasc Imaging Rep. 2011; 4(2):127–133.
16. Markl M, Kilner PJ, Ebbers T. Comprehensive 4D velocity mapping of the heart and great vessels by cardiovascular magnetic resonance. J Cardiovasc Magn Reson. 2011; 13(1):7. [PubMed: 21235751]
17. Frydrychowicz A, Francois CJ, Turski PA. Four-dimensional phase contrast magnetic resonance angiography: potential clinical applications. Eur J Radiol. 2011
18. Markl M, Frydrychowicz A, Kozerke S, Hope M, Wieben O. 4D flow MRI. J Magn Reson Imaging. 2012; 36(5):1015–1036. [PubMed: 23090914]
19. Hope MD, Sedlic T, Dyverfeldt P. Cardiothoracic magnetic resonance flow imaging. J Thorac Imaging. 2013; 28(4):217–230. [PubMed: 23708687]
20. Stankovic Z, Allen BD, Garcia J, Jarvis KB, Markl M. 4D flow imaging with MRI. Cardiovasc Diagn Ther. 2014; 4(2):173–192. [PubMed: 24834414]
21. Stalder AF, Russe MF, Frydrychowicz A, Bock J, Hennig J, Markl M. Quantitative 2D and 3D phase contrast MRI: optimized analysis of blood flow and vessel wall parameters. Magn Reson Med. 2008; 60(5):1218–1231. [PubMed: 18956416]

22. Bieging ET, Frydrychowicz A, Wentland A, et al. *In vivo* three-dimensional MR wall shear stress estimation in ascending aortic dilatation. J Magn Reson Imaging. 2011; 33(3):589–597. [PubMed: 21563242]
23. Potters WV, Ooij P, Marquering H, vanBavel E, Nederveen AJ. Volumetric arterial wall shear stress calculation based on cine phase contrast MRI. J Magn Reson Imaging. 2014:1–12.
24. Yang GZ, Kilner PJ, Wood NB, Underwood SR, Firmin DN. Computation of flow pressure fields from magnetic resonance velocity mapping. Magn Reson Med. 1996; 36(4):520–526. [PubMed: 8892202]
25. Tyszka JM, Laidlaw DH, Asa JW, Silverman JM. Three-dimensional, time-resolved (4D) relative pressure mapping using magnetic resonance imaging. J Magn Reson Imaging. 2000; 12(2):321–329. [PubMed: 10931596]
26. Ebbers T, Wigstrom L, Bolger AF, Engvall J, Karlsson M. Estimation of relative cardiovascular pressures using time-resolved three-dimensional phase contrast MRI. Magn Reson Med. 2001; 45(5):872–879. [PubMed: 11323814]
27. Ebbers T, Wigstrom L, Bolger AF, Wranne B, Karlsson M. Noninvasive measurement of time-varying three-dimensional relative pressure fields within the human heart. J Biomech Eng. 2002; 124(3):288–293. [PubMed: 12071263]
28. Lum DP, Johnson KM, Paul RK, et al. Transstenotic pressure gradients: measurement in swine—retrospectively ECG-gated 3D phase-contrast MR angiography versus endovascular pressure-sensing guidewires. Radiology. 2007; 245(3):751–760. [PubMed: 18024452]
29. Markl M, Wallis W, Brendecke S, Simon J, Frydrychowicz A, Harloff A. Estimation of global aortic pulse wave velocity by flow-sensitive 4D MRI. Magn Reson Med. 2010; 63(6):1575–1582. [PubMed: 20512861]
30. Wentland AL, Wieben O, Francois CJ, et al. Aortic pulse wave velocity measurements with undersampled 4D flow-sensitive MRI: comparison with 2D and algorithm determination. J Magn Reson Imaging. 2013; 37(4):853–859. [PubMed: 23124585]
31. Dyverfeldt P, Sigfridsson A, Kvitting JP, Ebbers T. Quantification of intravoxel velocity standard deviation and turbulence intensity by generalizing phase-contrast MRI. Magn Reson Med. 2006; 56(4):850–858. [PubMed: 16958074]
32. Dyverfeldt P, Gardhagen R, Sigfridsson A, Karlsson M, Ebbers T. On MRI turbulence quantification. Magn Reson Imaging. 2009; 27(7):913–922. [PubMed: 19525079]
33. Dyverfeldt P, Kvitting JP, Sigfridsson A, Engvall J, Bolger AF, Ebbers T. Assessment of fluctuating velocities in disturbed cardiovascular blood flow: *in vivo* feasibility of generalized phase-contrast MRI. J Magn Reson Imaging. 2008; 28(3):655–663. [PubMed: 18777557]
34. Binter C, Knobloch V, Manka R, Sigfridsson A, Kozerke S. Bayesian multipoint velocity encoding for concurrent flow and turbulence mapping. Magn Reson Med. 2013; 69(5):1337–1345. [PubMed: 22700280]
35. Eriksson J, Carlhall CJ, Dyverfeldt P, Engvall J, Bolger AF, Ebbers T. Semi-automatic quantification of 4D left ventricular blood flow. J Cardiovasc Magn Reson. 2010; 12(1):9. [PubMed: 20152026]
36. Eriksson J, Dyverfeldt P, Engvall J, Bolger AF, Ebbers T, Carlhäll CJ. Quantification of presystolic blood flow organization and energetics in the human left ventricle. Am J Physiol Heart Circ Physiol. 2011; 300(6):H2135–H2141. [PubMed: 21421820]
37. Sigovan M, Hope MD, Dyverfeldt P, Saloner D. Comparison of four-dimensional flow parameters for quantification of flow eccentricity in the ascending aorta. J Magn Reson Imaging. 2011; 34(5):1226–1230. [PubMed: 21928387]
38. Barker AJ, Ooij P, Bandi K, et al. Viscous energy loss in the presence of abnormal aortic flow. Magn Reson Med. Sep; 2014 72(3):620–8. Epub 2013 Oct 2. DOI: 10.1002/mrm.24962 [PubMed: 24122967]
39. Heiberg E, Ebbers T, Wigstrom L, Karlsson M. Three-dimensional flow characterization using vector pattern matching. IEEE Trans Vis Comput Graph. 2003; 9(3):313–319.
40. Toger J, Carlsson M, Soderlind G, Arheden H, Heiberg E. Volume Tracking: A new method for quantitative assessment and visualization of intracardiac blood flow from three-dimensional, time-

resolved, three-component magnetic resonance velocity mapping. BMC Med Imaging. 2011; 11:10. [PubMed: 21486430]

41. Töger J, Kanski M, Carlsson M, et al. Vortex ring formation in the left ventricle of the heart: analysis by 4D flow MRI and Lagrangian coherent structures. Ann Biomed Eng. 2012; 40(12): 2652–2662. [PubMed: 22805980]
42. Lustig M, Donoho D, Pauly JM. Sparse MRI: The application of compressed sensing for rapid MR imaging. Magn Reson Med. 2007; 58(6):1182–1195. [PubMed: 17969013]
43. Johnson KM, Lum DP, Turski PA, Block WF, Mistretta CA, Wieben O. Improved 3D phase contrast MRI with off-resonance corrected dual echo VIPR. Magn Reson Med. 2008; 60(6):1329–1336. [PubMed: 19025882]
44. Griswold MA, Jakob PM, Heidemann RM, et al. Generalized autocalibrating partially parallel acquisitions (GRAPPA). Magn Reson Med. 2002; 47(6):1202–1210. [PubMed: 12111967]
45. Baltes C, Kozerke S, Hansen MS, Pruessmann KP, Tsao J, Boesiger P. Accelerating cine phase-contrast flow measurements using k-t BLAST and k-t SENSE. Magn Reson Med. 2005; 54(6): 1430–1438. [PubMed: 16276492]
46. Jung B, Stalder AF, Bauer S, Markl M. On the undersampling strategies to accelerate time-resolved 3D imaging using k-t-GRAPPA. Magn Reson Med. 2011; 66(4):966–975. [PubMed: 21437975]
47. Giese D, Schaeffter T, Kozerke S. Highly undersampled phase-contrast flow measurements using compartment-based k-t principal component analysis. Magn Reson Med. 2013; 69(2):434–443. [PubMed: 22528878]
48. Tsao J, Kozerke S. MRI temporal acceleration techniques. J Magn Reson Imaging. 2012; 36(3): 543–560. [PubMed: 22903655]
49. Schnell S, Markl M, Entezari P, et al. k-t GRAPPA accelerated four-dimensional flow MRI in the aorta: effect on scan time, image quality, and quantification of flow and wall shear stress. Magn Reson Med. 2014; 72(2):522–533. [PubMed: 24006309]
50. Stankovic Z, Fink J, Collins JD, et al. k-t GRAPPA-accelerated 4D flow MRI of liver hemodynamics: influence of different acceleration factors on qualitative and quantitative assessment of blood flow. MAGMA. Apr; 2015 28(2):149–59. Epub 2014 Aug 7. DOI: 10.1007/s10334-014-0456-1 [PubMed: 25099493]
51. Hsiao A, Lustig M, Alley MT, Murphy MJ, Vasanawala SS. Evaluation of valvular insufficiency and shunts with parallel-imaging compressed-sensing 4D phase-contrast MR imaging with stereoscopic 3D velocity-fusion volume-rendered visualization. Radiology. 2012; 265(1):87–95. [PubMed: 22923717]
52. Chai P, Mohiaddin R. How we perform cardiovascular magnetic resonance flow assessment using phase-contrast velocity mapping. J Cardiovasc Magn Reson. 2005; 7(4):705–716. [PubMed: 16136862]
53. Mohiaddin RH, Yang GZ, Kilner PJ. Visualization of flow by vector analysis of multidirectional cine MR velocity mapping. J Comp Assist Tomogr. 1994; 18(3):383–392.
54. Brix L, Ringgaard S, Rasmusson A, Sorensen TS, Kim WY. Three dimensional three component whole heart cardiovascular magnetic resonance velocity mapping: comparison of flow measurements from 3D and 2D acquisitions. J Cardiovasc Magn Reson. 2009; 11:3. [PubMed: 19232119]
55. Carlsson M, Toger J, Kanski M, et al. Quantification and visualization of cardiovascular 4D velocity mapping accelerated with parallel imaging or k-t BLAST: head to head comparison and validation at 1.5 T and 3 T. J Cardiovasc Magn Reson. 2011; 13:55. [PubMed: 21970399]
56. Eriksson J, Carlhall CJ, Dyverfeldt P, Engvall J, Bolger AF, Ebbers T. Semi-automatic quantification of 4D left ventricular blood flow. J Cardiovasc Magn Reson. 2010; 12:9. [PubMed: 20152026]
57. Frydrychowicz A, Wieben O, Niespodzany E, Reeder SB, Johnson KM, Francois CJ. Quantification of thoracic blood flow using volumetric magnetic resonance imaging with radial velocity encoding: *in vivo* validation. Invest Radiol. 2013; 48(12):819–825. [PubMed: 23857136]
58. Gabbour M, Schnell S, Jarvis K, Robinson JD, Markl M, Rigsby CK. D flow magnetic resonance imaging: blood flow quantification compared to 2-D phase-contrast magnetic resonance imaging and Doppler echocardiography. Pediatr Radiol. 2015; 45(6):804–813. [PubMed: 25487721]

59. Hanneman K, Sivagnanam M, Nguyen ET, et al. Magnetic resonance assessment of pulmonary (QP) to systemic (QS) flows using 4D phase-contrast imaging: pilot study comparison with standard through-plane 2D phase-contrast imaging. Acad Radiol. 2014; 21(8):1002–1008. [PubMed: 25018072]
60. Hope MD, Meadows AK, Hope TA, et al. Clinical evaluation of aortic coarctation with 4D flow MR imaging. J Magn Reson Imaging. 2010; 31(3):711–718. [PubMed: 20187217]
61. Hsiao A, Alley MT, Massaband P, Herfkens RJ, Chan FP, Vasanawala SS. Improved cardiovascular flow quantification with time-resolved volumetric phase-contrast MRI. Pediatr Radiol. 2011; 41(6):711–720. [PubMed: 21221566]
62. Markl M, Chan FP, Alley MT, et al. Time-resolved three-dimensional phase-contrast MRI. J Magn Reson Imaging. 2003; 17(4):499–506. [PubMed: 12655592]
63. Meckel S, Leitner L, Bonati LH, et al. Intracranial artery velocity measurement using 4D PC MRI at 3 T: comparison with transcranial ultrasound techniques and 2D PC MRI. Neuroradiology. 2013; 55(4):389–398. [PubMed: 23143179]
64. Nordmeyer S, Riesenkampff E, Crelier G, et al. Flow-sensitive four-dimensional cine magnetic resonance imaging for offline blood flow quantification in multiple vessels: a validation study. J Magn Reson Imaging. 2010; 32(3):677–683. [PubMed: 20815066]
65. Nordmeyer S, Riesenkampff E, Messroghli D, et al. Four-dimensional velocity-encoded magnetic resonance imaging improves blood flow quantification in patients with complex accelerated flow. J Magn Reson Imaging. 2013; 37(1):208–216. [PubMed: 22976284]
66. Uribe S, Beerbaum P, Sorensen TS, Rasmusson A, Razavi R, Schaeffter T. Four-dimensional (4D) flow of the whole heart and great vessels using real-time respiratory self-gating. Magn Reson Med. 2009; 62(4):984–992. [PubMed: 19672940]
67. Valverde I, Nordmeyer S, Uribe S, et al. Systemic-to-pulmonary collateral flow in patients with palliated univentricular heart physiology: measurement using cardiovascular magnetic resonance 4D velocity acquisition. J Cardiovasc Magn Reson. 2012; 14:25. [PubMed: 22541134]
68. van der Hulst AE, Westenberg JJ, Kroft LJ, et al. Tetralogy of fallot: 3D velocity-encoded MR imaging for evaluation of right ventricular valve flow and diastolic function in patients after correction. Radiology. 2010; 256(3):724–734. [PubMed: 20634432]
69. Wentland AL, Grist TM, Wieben O. Repeatability and internal consistency of abdominal 2D and 4D phase contrast MR flow measurements. Acad Radiol. 2013; 20(6):699–704. [PubMed: 23510798]
70. Zaman A, Motwani M, Oliver JJ, et al. 3.0T, time-resolved, 3D flow-sensitive MR in the thoracic aorta: impact of k-t BLAST acceleration using 8- versus 32-channel coil arrays. J Magn Reson Imaging. 2015; 42(2):495–504. [PubMed: 25447784]
71. Ehman RL, Felmlee JP. Adaptive technique for high-definition MR imaging of moving structures. Radiology. 1989; 173(1):255–263. [PubMed: 2781017]
72. McConnell MV, Khasgiwala VC, Savord BJ, et al. Comparison of respiratory suppression methods and navigator locations for MR coronary angiography. AJR Am J Roentgenol. 1997; 168(5):1369–1375. [PubMed: 9129447]
73. Wang Y, Rossman PJ, Grimm RC, Riederer SJ, Ehman RL. Navigator-echo-based real-time respiratory gating and triggering for reduction of respiration effects in three-dimensional coronary MR angiography. Radiology. 1996; 198(1):55–60. [PubMed: 8539406]
74. Baltes C, Kozerke S, Atkinson D, Boesiger P. Retrospective respiratory motion correction for navigated cine velocity mapping. J Cardiovasc Magn Reson. 2004; 6(4):785–792. [PubMed: 15646881]
75. Larson AC, White RD, Laub G, McVeigh ER, Li D, Simonetti OP. Self-gated cardiac cine MRI. Magn Reson Med. 2004; 51(1):93–102. [PubMed: 14705049]
76. Buehrer M, Curcic J, Boesiger P, Kozerke S. Prospective self-gating for simultaneous compensation of cardiac and respiratory motion. Magn Reson Med. 2008; 60(3):683–690. [PubMed: 18727084]
77. Uribe S, Muthurangu V, Boubertakh R, et al. Whole-heart cine MRI using real-time respiratory self-gating. Magn Reson Med. 2007; 57(3):606–613. [PubMed: 17326164]

78. Stehning C, Bornert P, Nehrke K, Eggers H, Stuber M. Free-breathing wholeheart coronary MRA with 3D radial SSFP and self-navigated image reconstruction. Magn Reson Med. 2005; 54(2):476–480. [PubMed: 16032682]

79. Winkelmann S, Schaeffter T, Koehler T, Eggers H, Doessel O. An optimal radial profile order based on the Golden Ratio for time-resolved MRI. IEEE Trans Med Imaging. 2007; 26(1):68–76. [PubMed: 17243585]

80. Batchelor PG, Atkinson D, Irarrazaval P, Hill DL, Hajnal J, Larkman D. Matrix description of general motion correction applied to multishot images. Magn Reson Med. 2005; 54(5):1273–1280. [PubMed: 16155887]

81. Odille F, Vuissoz PA, Marie PY, Felblinger J. Generalized reconstruction by inversion of coupled systems (GRICS) applied to free-breathing MRI. Magn Reson Med. 2008; 60(1):146–157. [PubMed: 18581355]

82. Bauer S, Markl M, Foll D, Russe M, Stankovic Z, Jung B. k-t GRAPPA accelerated phase contrast MRI: Improved assessment of blood flow and 3-directional myocardial motion during breath-hold. J Magn Reson Imaging. 2013; 38(5):1054–1062. [PubMed: 23908094]

83. Dyvorne H, Knight-Greenfield A, Jajamovich G, et al. Abdominal 4D flow MR imaging in a breath hold: combination of spiral sampling and dynamic compressed sensing for highly accelerated acquisition. Radiology. 2015; 275(1):245–254. [PubMed: 25325326]

84. Frydrychowicz A, Stalder AF, Russe MF, et al. Three-dimensional analysis of segmental wall shear stress in the aorta by flow-sensitive four-dimensional-MRI. J Magn Reson Imaging. 2009; 30(1): 77–84. [PubMed: 19557849]

85. Isoda H, Ohkura Y, Kosugi T, et al. Comparison of hemodynamics of intracranial aneurysms between MR fluid dynamics using 3D cine phase-contrast MRI and MR-based computational fluid dynamics. Neuroradiology. 2010; 52(10):913–920. [PubMed: 19967532]

86. Hope MD, Hope TA, Crook SE, et al. 4D flow CMR in assessment of valve-related ascending aortic disease. JACC Cardiovasc Imaging. 2011; 4(7):781–787. [PubMed: 21757170]

87. Barker AJ, Markl M, Burk J, et al. Bicuspid aortic valve is associated with altered wall shear stress in the ascending aorta. Circ Cardiovasc Imaging. 2012; 5(4):457–466. [PubMed: 22730420]

88. Burk J, Blanke P, Stankovic Z, et al. Evaluation of 3D blood flow patterns and wall shear stress in the normal and dilated thoracic aorta using flow-sensitive 4D CMR. J Cardiovasc Magn Reson. 2012; 14:84. [PubMed: 23237187]

89. Geiger J, Arnold R, Herzer L, et al. Aortic wall shear stress in Marfan syndrome. Magn Reson Med. Oct; 2013 70(4):1137–44. Epub 2012 Nov 20. DOI: 10.1002/mrm.24562 [PubMed: 23169240]

90. Moftakhar R, Aagaard-Kienitz B, Johnson K, et al. Noninvasive measurement of intra-aneurysmal pressure and flow pattern using phase contrast with vastly undersampled isotropic projection imaging. AJNR Am J Neuroradiol. 2007; 28(9):1710–1714. [PubMed: 17885239]

91. Bley TA, Johnson KM, Francois CJ, et al. Noninvasive assessment of transstenotic pressure gradients in porcine renal artery stenoses by using vastly undersampled phase-contrast MR angiography. Radiology. 2011; 261(1):266–273. [PubMed: 21813739]

92. Bock J, Frydrychowicz A, Lorenz R, et al. *In vivo* noninvasive 4D pressure difference mapping in the human aorta: phantom comparison and application in healthy volunteers and patients. Magn Reson Med. 2011; 66(4):1079–1088. [PubMed: 21437978]

93. Kvitting JP, Dyverfeldt P, Sigfridsson A, et al. In vitro assessment of flow patterns and turbulence intensity in prosthetic heart valves using generalized phase-contrast MRI. J Magn Reson Imaging. 2010; 31(5):1075–1080. [PubMed: 20432341]

94. Hsiao A, Tariq U, Alley MT, Lustig M, Vasanawala SS. Inlet and outlet valve flow and regurgitant volume may be directly and reliably quantified with accelerated, volumetric phase-contrast MRI. J Magn Reson Imaging. 2015; 41(2):376–385. [PubMed: 24677253]

95. Mahadevia R, Barker AJ, Schnell S, et al. Bicuspid aortic cusp fusion morphology alters aortic three-dimensional outflow patterns, wall shear stress, and expression of aortopathy. Circulation. 2014; 129(6):673–682. [PubMed: 24345403]

96. Francois CJ, Markl M, Schiebler ML, et al. Four-dimensional, flow-sensitive magnetic resonance imaging of blood flow patterns in thoracic aortic dissections. J Thorac Cardiovasc Surg. 2013; 145(5):1359–1366. [PubMed: 22841438]

97. Riesenkampff E, Fernandes JF, Meier S, et al. Pressure fields by flow-sensitive, 4D, velocity-encoded CMR in patients with aortic coarctation. JACC Cardiovasc Imaging. 2014; 7(9):920–926. [PubMed: 25212797]

98. Bane O, Shah SJ, Cuttica MJ, et al. A non-invasive assessment of cardiopulmonary hemodynamics with MRI in pulmonary hypertension. Magn Reson Imaging. Dec; 2015 33(10):1224–35. Epub 2015 Aug 14. DOI: 10.1016/j.mri.2015.08.005 [PubMed: 26283577]

99. Bollache E, Kachenoura N, Bargiotas I, et al. How to estimate aortic characteristic impedance from magnetic resonance and applanation tonometry data? J Hypertension. 2015; 33(3):575–582. discussion 583.

100. Chen SS, Kilner PJ. Unilateral pulmonary artery branch stenosis: diastolic prolongation of forward flow appears to maintain flow to the affected lung if the pulmonary valve is competent. Int J Cardiol. 2013; 168(4):3698–3703. [PubMed: 23849966]

101. Defrance C, Bollache E, Kachenoura N, et al. Evaluation of aortic valve stenosis using cardiovascular magnetic resonance: comparison of an original semiautomated analysis of phase-contrast cardiovascular magnetic resonance with Doppler echocardiography. Circ Cardiovasc Imaging. 2012; 5(5):604–612. [PubMed: 22798520]

102. Garcia J, Markl M, Schnell S, et al. Evaluation of aortic stenosis severity using 4D flow jet shear layer detection for the measurement of valve effective orifice area. Magn Reson Imaging. 2014; 32(7):891–898. [PubMed: 24865143]

103. Bargiotas I, Mousseaux E, Yu WC, et al. Estimation of aortic pulse wave transit time in cardiovascular magnetic resonance using complex wavelet cross-spectrum analysis. J Cardiovasc Magn Reson. 2015; 17(1):65. [PubMed: 26219835]

104. Dyverfeldt P, Ebbers T, Lanne T. Pulse wave velocity with 4D flow MRI: systematic differences and age-related regional vascular stiffness. Magn Reson Imaging. 2014; 32(10):1266–1271. [PubMed: 25171817]

105. Guzzardi DG, Barker AJ, van Ooij P, et al. Valve-related hemodynamics mediate human bicuspid aortopathy: insights from wall shear stress mapping. J Am Coll Cardiol. 2015; 66(8):892–900. [PubMed: 26293758]

106. van Ooij P, Potters WV, Collins J, et al. Characterization of abnormal wall shear stress using 4D flow MRI in human bicuspid aortopathy. Ann Biomed Eng. 2015; 43(6):1385–1397. [PubMed: 25118671]

107. Oshinski JN, Ku DN, Mukundan S Jr. Loth F, Pettigrew RI. Determination of wall shear stress in the aorta with the use of MR phase velocity mapping. J Magn Reson Imaging. 1995; 5(6):640–647. [PubMed: 8748480]

108. Oyre S, Paaske WP, Ringgaard S, et al. Automatic accurate non-invasive quantitation of blood flow, cross-sectional vessel area, and wall shear stress by modelling of magnetic resonance velocity data. Eur J Vasc Endovasc Surg. 1998; 16(6):517–524. [PubMed: 9894493]

109. Boussel L, Rayz V, Martin A, et al. Phase-contrast magnetic resonance imaging measurements in intracranial aneurysms *in vivo* of flow patterns, velocity fields, and wall shear stress: comparison with computational fluid dynamics. Magn Reson Med. 2009; 61(2):409–417. [PubMed: 19161132]

110. Kozerke S, Scheidegger MB, Pedersen EM, Boesiger P. Heart motion adapted cine phase-contrast flow measurements through the aortic valve. Magn Reson Med. 1999; 42(5):970–978. [PubMed: 10542357]

111. Roes SD, Hammer S, van der Geest RJ, et al. Flow assessment through four heart valves simultaneously using 3-dimensional 3-directional velocity-encoded magnetic resonance imaging with retrospective valve tracking in healthy volunteers and patients with valvular regurgitation. Invest Radiol. 2009; 44(10):669–675. [PubMed: 19724233]

112. Hoffman JI, Kaplan S. The incidence of congenital heart disease. J Am Coll Cardiol. 2002; 39(12):1890–1900. [PubMed: 12084585]

113. Roberts WC. The congenitally bicuspid aortic valve. A study of 85 autopsy cases. Am J Cardiol. 1970; 26(1):72–83. [PubMed: 5427836]
114. Basso C, Boschello M, Perrone C, et al. An echocardiographic survey of primary school children for bicuspid aortic valve. Am J Cardiol. 2004; 93(5):661–663. [PubMed: 14996606]
115. Roger VL, Go AS, Lloyd-Jones DM, et al. Heart disease and stroke statistics—2011 update: a report from the American Heart Association. Circulation. 2011; 123(4):e18–e209. [PubMed: 21160056]
116. Hope MD, Hope TA, Meadows AK, et al. Bicuspid aortic valve: four-dimensional MR evaluation of ascending aortic systolic flow patterns. Radiology. 2010; 255(1):53–61. [PubMed: 20308444]
117. Barker AJ, Markl M, Bürk J, et al. Bicuspid aortic valve is associated with altered wall shear stress in the ascending aortaclinical perspective. Circ Cardiovasc Imaging. 2012; 5(4):457–466. [PubMed: 22730420]
118. Meierhofer C, Schneider EP, Lyko C, et al. Wall shear stress and flow patterns in the ascending aorta in patients with bicuspid aortic valves differ significantly from tricuspid aortic valves: a prospective study. Eur Heart J Cardiovasc Imaging. 2012
119. Bissell MM, Hess AT, Biasiolli L, et al. Aortic dilation in bicuspid aortic valve disease: flow pattern is a major contributor and differs with valve fusion type. Circ Cardiovasc Imaging. 2013; 6(4):499–507. [PubMed: 23771987]
120. Hope MD, Sigovan M, Wrenn SJ, Saloner D, Dyverfeldt P. MRI hemodynamic markers of progressive bicuspid aortic valve-related aortic disease. J Magn Reson Imaging. 2014; 40(1):140–145. [PubMed: 24788592]
121. Amarenco P, Cohen A, Tzourio C, et al. Atherosclerotic disease of the aortic arch and the risk of ischemic stroke. N Engl J Med. 1994; 331(22):1474–1479. [PubMed: 7969297]
122. Reimold SC, Maier SE, Aggarwal K, et al. Aortic flow velocity patterns in chronic aortic regurgitation: implications for Doppler echocardiography. J Am Soc Echocardiogr. 1996; 9(5): 675–683. [PubMed: 8887871]
123. Kronzon I, Tunick PA. Aortic atherosclerotic disease and stroke. Circulation. 2006; 114(1):63–75. [PubMed: 16818829]
124. Bogren HG, Mohiaddin RH, Kilner PJ, Jimenez-Borreguero LJ, Yang GZ, Firmin DN. Blood flow patterns in the thoracic aorta studied with three-directional MR velocity mapping: the effects of age and coronary artery disease. J Magn Reson Imaging. 1997; 7(5):784–793. [PubMed: 9307902]
125. Bogren HG, Buonocore MH, Valente RJ. Four-dimensional magnetic resonance velocity mapping of blood flow patterns in the aorta in patients with atherosclerotic coronary artery disease compared to age-matched normal subjects. J Magn Reson Imaging. 2004; 19(4):417–427. [PubMed: 15065165]
126. Harloff A, Strecker C, Frydrychowicz AP, et al. Plaques in the descending aorta: a new risk factor for stroke? Visualization of potential embolization pathways by 4D MRI. J Magn Reson Imaging. 2007; 26(6):1651–1655. [PubMed: 18022846]
127. Harloff A, Simon J, Brendecke S, et al. Complex plaques in the proximal descending aorta: an underestimated embolic source of stroke. Stroke. 2010; 41(6):1145–1150. [PubMed: 20431080]
128. Barker AJ, Roldan-Alzate A, Entezari P, et al. Four-dimensional flow assessment of pulmonary artery flow and wall shear stress in adult pulmonary arterial hypertension: results from two institutions. Magn Reson Med. 2015; 73(5):1904–1913. [PubMed: 24974951]
129. Truong U, Fonseca B, Dunning J, et al. Wall shear stress measured by phase contrast cardiovascular magnetic resonance in children and adolescents with pulmonary arterial hypertension. J Cardiovasc Magn Reson. 2013; 15:81. [PubMed: 24034144]
130. Reiter G, Reiter U, Kovacs G, et al. Magnetic resonance derived 3-dimensional blood flow patterns in the main pulmonary artery as a marker of pulmonary hypertension and a measure of elevated mean pulmonary arterial pressure. Circ Cardiovasc Imaging. 2008; 1:23–30. [PubMed: 19808511]
131. Reiter U, Reiter G, Kovacs G, et al. Evaluation of elevated mean pulmonary arterial pressure based on magnetic resonance 4D velocity mapping: comparison of visualization techniques. PLoS One. 2013; 8(12):e82212. [PubMed: 24349224]

132. van der Linde D, Konings EE, Slager MA, et al. Birth prevalence of congenital heart disease worldwide: a systematic review and meta-analysis. J Am Coll Cardiol. 2011; 58(21):2241–2247. [PubMed: 22078432]
133. Hoffman J, Kaplan S. The incidence of congenital heart disease. J Am Coll Cardiol. 2002; 39(12): 1890–1900. [PubMed: 12084585]
134. Kathiria NN, Higgins CB, Ordovas KG. Advances in MR imaging assessment of adults with congenital heart disease. Magn Reson Imaging Clin N Am. 2015; 23(1):35–40. [PubMed: 25476672]
135. Helbing WA, Ouhlous M. Cardiac magnetic resonance imaging in children. Pediatr Radiol. 2015; 45(1):20–26. [PubMed: 25552387]
136. Weber OM, Higgins CB. MR evaluation of cardiovascular physiology in congenital heart disease: flow and function. J Cardiovasc Magn Reson. 2006; 8(4):607–617. [PubMed: 16869313]
137. Sorensen TS, Beerbaum P, Korperich H, Pedersen EM. Three-dimensional, isotropic MRI: a unified approach to quantification and visualization in congenital heart disease. Int J Cardiovasc Imaging. 2005; 21(2-3):283–292. [PubMed: 16015442]
138. Varaprasathan GA, Araoz PA, Higgins CB, Reddy GP. Quantification of flow dynamics in congenital heart disease: applications of velocity-encoded cine MR imaging. RadioGraphics. 2002; 22(4):895–905. discussion 905-896. [PubMed: 12110719]
139. Rebergen SA, de Roos A. Congenital heart disease. Evaluation of anatomy and function by MRI. Herz. 2000; 25(4):365–383. [PubMed: 10948773]
140. Kilner PJ, Gatehouse PD, Firmin DN. Flow measurement by magnetic resonance: a unique asset worth optimising. J Cardiovasc Magn Reson. 2007; 9(4):723–728. [PubMed: 17613655]
141. Odegard KC, DiNardo JA, Tsai-Goodman B, Powell AJ, Geva T, Laussen PC. Anaesthesia considerations for cardiac MRI in infants and small children. Paediatr Anaesth. 2004; 14(6):471–476. [PubMed: 15153209]
142. Fogel MA, Weinberg PM, Parave E, et al. Deep sedation for cardiac magnetic resonance imaging: a comparison with cardiac anesthesia. J Pediatr. 2008; 152(4):534–539. 539, e531. [PubMed: 18346511]
143. Driessen MM, Breur JM, Budde RP, et al. Advances in cardiac magnetic resonance imaging of congenital heart disease. Pediatr Radiol. 2015; 45(1):5–19. [PubMed: 25552386]
144. Orwat S, Diller GP, Baumgartner H. Imaging of congenital heart disease in adults: choice of modalities. Eur Heart J Cardiovasc Imaging. 2014; 15(1):6–17. [PubMed: 23913331]
145. Fredenburg TB, Johnson TR, Cohen MD. The Fontan procedure: anatomy, complications, and manifestations of failure. RadioGraphics. 2011; 31(2):453–463. [PubMed: 21415190]
146. Cordina RL, O'Meagher S, Karmali A, et al. Resistance training improves cardiac output, exercise capacity and tolerance to positive airway pressure in Fontan physiology. Int J Cardiol. 2013; 168(2):780–788. [PubMed: 23154055]
147. Korperich H, Barth P, Gieseke J, et al. Impact of respiration on stroke volumes in paediatric controls and in patients after Fontan procedure assessed by MR real-time phase-velocity mapping. Eur Heart J Cardiovasc Imaging. 2015; 16(2):198–209. [PubMed: 25246504]
148. O'Meagher S, Munoz PA, Muthurangu V, et al. Mechanisms of maintained exercise capacity in adults with repaired tetralogy of Fallot. Int J Cardiol. 2014; 177(1):178–181. [PubMed: 25499372]
149. Geiger J, Markl M, Jung B, et al. 4D-MR flow analysis in patients after repair for tetralogy of Fallot. Eur Radiol. 2011; 21(8):1651–1657. [PubMed: 21720942]
150. Francois CJ, Srinivasan S, Schiebler ML, et al. 4D cardiovascular magnetic resonance velocity mapping of alterations of right heart flow patterns and main pulmonary artery hemodynamics in tetralogy of Fallot. J Cardiovasc Magn Reson. 2012; 14:16. [PubMed: 22313680]
151. Markl M, Geiger J, Kilner PJ, et al. Time-resolved three-dimensional magnetic resonance velocity mapping of cardiovascular flow paths in volunteers and patients with Fontan circulation. Eur J Cardiothorac Surg. 2011; 39(2):206–212. [PubMed: 20598560]
152. Vasanawala SS, Hanneman K, Alley MT, Hsiao A. Congenital heart disease assessment with 4D flow MRI. J Magn Reson Imaging. 2015

153. Goldman ME, Pearce LA, Hart RG, et al. Pathophysiologic correlates of thromboembolism in nonvalvular atrial fibrillation: I. Reduced flow velocity in the left atrial appendage (The Stroke Prevention in Atrial Fibrillation [SPAF-III] study). J Am Soc Echocardiogr. 1999; 12(12):1080–1087. [PubMed: 10588784]

154. Handke M, Harloff A, Hetzel A, Olschewski M, Bode C, Geibel A. Left atrial appendage flow velocity as a quantitative surrogate parameter for thromboembolic risk: determinants and relationship to spontaneous echocontrast and thrombus formation—a transesophageal echocardiographic study in 500 patients with cerebral ischemia. J Am Soc Echocardiogr. 2005; 18(12):1366–1372. [PubMed: 16376768]

155. Pollick C, Taylor D. Assessment of left atrial appendage function by transesophageal echocardiography. Implications for the development of thrombus. Circulation. 1991; 84(1):223–231. [PubMed: 2060098]

156. Lee, D.; Goldberger, J.; Fluckiger, J., et al. Analysis of left atrial flow velocity distribution by 4D flow MRI in patients with atrial fibrillation. Dallas, Tx: 2013.

157. Goldberger, J.; Fluckiger, J.; Lee, D., et al. Left atrial flow velocity distribution in atrial fibrillation by 4D flow MRI: a new marker for risk of stroke?. Denver, CO; USA: 2013.

158. Fluckiger JU, Goldberger JJ, Lee DC, et al. Left atrial flow velocity distribution and flow coherence using four-dimensional FLOW MRI: a pilot study investigating the impact of age and pre- and postintervention atrial fibrillation on atrial hemodynamics. J Magn Reson Imaging. 2013; 38(3):580–587. [PubMed: 23292793]

159. Markl M, Lee DC, Ng J, Carr M, Carr J, Goldberger JJ. Left atrial 4-dimensional flow magnetic resonance imaging: stasis and velocity mapping in patients with atrial fibrillation. Invest Radiol. Oct 20.2015 [Epub ahead of print].

160. Lee DC, Markl M, Ng J, et al. Three-dimensional left atrial blood flow characteristics in patients with atrial fibrillation assessed by 4D flow CMR. Eur Heart J Cardiovasc Imaging. Nov 20.2015 :pii: jev304. [Epub ahead of print].

161. Kowallick JT, Joseph AA, Unterberg-Buchwald C, et al. Real-time phase-contrast flow MRI of the ascending aorta and superior vena cava as a function of intrathoracic pressure (Valsalva manoeuvre). Br J Radiol. 2014; 87(1042):20140401. [PubMed: 25074791]

162. Thavendiranathan P, Verhaert D, Walls MC, et al. Simultaneous right and left heart real-time, free-breathing CMR flow quantification identifies constrictive physiology. JACC Cardiovasc imaging. 2012; 5(1):15–24. [PubMed: 22239888]

163. Kellman P, Epstein FH, McVeigh ER. Adaptive sensitivity encoding incorporating temporal filtering (TSENSE). Magn Reson Med. 2001; 45(5):846–852. [PubMed: 11323811]

164. Brandts A, Roes SD, Doornbos J, et al. Right coronary artery flow velocity and volume assessment with spiral k-space sampled breathhold velocity-encoded MRI at 3 tesla: accuracy and reproducibility. J Magn Reson Imaging. 2010; 31(5):1215–1223. [PubMed: 20432359]

165. Keegan J, Gatehouse P, Yang GZ, Firmin D. Interleaved spiral cine coronary artery velocity mapping. Magn Reson Med. 2000; 43(6):787–792. [PubMed: 10861871]

166. Johnson K, Sharma P, Oshinski J. Coronary artery flow measurement using navigator echo gated phase contrast magnetic resonance velocity mapping at 3.0 T. J Biomech. 2008; 41(3):595–602. [PubMed: 18036532]

167. Keegan J, Gatehouse PD, Mohiaddin RH, Yang GZ, Firmin DN. Comparison of spiral and FLASH phase velocity mapping, with and without breath-holding, for the assessment of left and right coronary artery blood flow velocity. J Magn Reson Imaging. 2004; 19(1):40–49. [PubMed: 14696219]

168. Nagel E, Thouet T, Klein C, et al. Noninvasive determination of coronary blood flow velocity with cardiovascular magnetic resonance in patients after stent deployment. Circulation. 2003; 107(13):1738–1743. [PubMed: 12665488]

169. Schwitter J, DeMarco T, Kneifel S, et al. Magnetic resonance-based assessment of global coronary flow and flow reserve and its relation to left ventricular functional parameters: a comparison with positron emission tomography. Circulation. 2000; 101(23):2696–2702. [PubMed: 10851206]

170. Saito Y, Sakuma H, Shibata M, et al. Assessment of coronary flow velocity reserve using fast velocity-encoded cine MRI for noninvasive detection of restenosis after coronary stent implantation. J Cardiovasc Magn Reson. 2001; 3(3):209–214. [PubMed: 11816617]
171. Hays AG, Kelle S, Hirsch GA, et al. Regional coronary endothelial function is closely related to local early coronary atherosclerosis in patients with mild coronary artery disease: pilot study. Circ Cardiovasc Imaging. 2012; 5(3):341–348. [PubMed: 22492483]
172. Jahnke C, Manka R, Kozerke S, et al. Cardiovascular magnetic resonance profiling of coronary atherosclerosis: vessel wall remodelling and related myocardial blood flow alterations. Eur Heart J Cardiovasc Imaging. 2014; 15(12):1400–1410. [PubMed: 25104810]
173. Kang CK, Park CA, Lee DS, et al. Velocity measurement of microvessels using phase-contrast magnetic resonance angiography at 7 tesla MRI. Magn Reson Med. May 15.2015 [Epub ahead of print]. doi: 10.1002/mrm.25600
174. Norgaard BL, Leipsic J, Gaur S, et al. Diagnostic performance of noninvasive fractional flow reserve derived from coronary computed tomography angiography in suspected coronary artery disease: the NXT trial (Analysis of Coronary Blood Flow Using CT Angiography: Next Steps). J Am Coll Cardiol. 2014; 63(12):1145–1155. [PubMed: 24486266]
175. Taylor CA, Fonte TA, Min JK. Computational fluid dynamics applied to cardiac computed tomography for noninvasive quantification of fractional flow reserve: scientific basis. J Am Coll Cardiol. 2013; 61(22):2233–2241. [PubMed: 23562923]
176. Schubert T, Bieri O, Pansini M, Stippich C, Santini F. Peak velocity measurements in tortuous arteries with phase contrast magnetic resonance imaging: the effect of multidirectional velocity encoding. Invest Radiol. 2014; 49(4):189–194. [PubMed: 24300842]
177. Liu P, Lu H, Filbey FM, et al. Automatic and reproducible positioning of phase-contrast MRI for the quantification of global cerebral blood flow. PloS one. 2014; 9(5):e95721. [PubMed: 24787742]
178. Gonzalez CF, Cho YI, Ortega HV, Moret J. Intracranial aneurysms: flow analysis of their origin and progression. AJNR Am J Neuroradiol. 1992; 13(1):181–188. [PubMed: 1595440]
179. Steinman DA, Milner JS, Norley CJ, Lownie SP, Holdsworth DW. Image-based computational simulation of flow dynamics in a giant intracranial aneurysm. AJNR Am J Neuroradiol. 2003; 24(4):559–566. [PubMed: 12695182]
180. Ohta M, Wetzel SG, Dantan P, et al. Rheological changes after stenting of a cerebral aneurysm: a finite element modeling approach. Cardiovasc Interv Radiol. 2005; 28(6):768–772.
181. Cebral JR, Castro MA, Appanaboyina S, Putman CM, Millan D, Frangi AF. Efficient pipeline for image-based patient-specific analysis of cerebral aneurysm hemodynamics: technique and sensitivity. IEEE Trans Med Imaging. 2005; 24(4):457–467. [PubMed: 15822804]
182. Cebral JR, Mut F, Weir J, Putman CM. Association of hemodynamic characteristics and cerebral aneurysm rupture. AJNR Am J Neuroradiol. 2011; 32(2):264–270. [PubMed: 21051508]
183. Sforza DM, Putman CM, Cebral JR. Hemodynamics of cerebral aneurysms. Ann Rev Fluid Mech. 2009; 41:91–107. [PubMed: 19784385]
184. Jou LD, Quick CM, Young WL, et al. Computational approach to quantifying hemodynamic forces in giant cerebral aneurysms. AJNR Am J Neuroradiol. 2003; 24(9):1804–1810. [PubMed: 14561606]
185. Rayz VL, Boussel L, Ge L, et al. Flow residence time and regions of intraluminal thrombus deposition in intracranial aneurysms. Ann Biomed Eng. 2010; 38(10):3058–3069. [PubMed: 20499185]
186. Jou LD, Wong G, Dispensa B, et al. Correlation between lumenal geometry changes and hemodynamics in fusiform intracranial aneurysms. AJNR Am J Neuroradiol. 2005; 26(9):2357–2363. [PubMed: 16219845]
187. Xiang J, Natarajan SK, Tremmel M, et al. Hemodynamic–morphologic discriminants for intracranial aneurysm rupture. Stroke. 2011; 42(1):144–152. [PubMed: 21106956]
188. Cebral JR, Castro MA, Burgess JE, Pergolizzi RS, Sheridan MJ, Putman CM. Characterization of cerebral aneurysms for assessing risk of rupture by using patient-specific computational hemodynamics models. AJNR Am J Neuroradiol. 2005; 26(10):2550–2559. [PubMed: 16286400]

189. Hassan T, Ezura M, Timofeev EV, et al. Computational simulation of therapeutic parent artery occlusion to treat giant vertebrobasilar aneurysm. AJNR Am J Neuroradiol. 2004; 25(1):63–68. [PubMed: 14729530]

190. van Ooij P, Potters WV, Guedon A, et al. Wall shear stress estimated with phase contrast MRI in an *in vitro* and *in vivo* intracranial aneurysm. J Magn Reson Imaging. 2013; 38(4):876–884. [PubMed: 23417769]

191. Tateshima S, Murayama Y, Villablanca JP, et al. *In vitro* measurement of fluid-induced wall shear stress in unruptured cerebral aneurysms harboring blebs. Stroke. 2003; 34(1):187–192. [PubMed: 12511772]

192. Castro MA, Putman CM, Cebral JR. Computational fluid dynamics modeling of intracranial aneurysms: effects of parent artery segmentation on intra-aneurysmal hemodynamics. AJNR Am J Neuroradiol. 2006; 27(8):1703–1709. [PubMed: 16971618]

193. Wetzel S, Meckel S, Frydrychowicz A, et al. *In vivo* assessment and visualization of intracranial arterial hemodynamics with flow-sensitized 4D MR imaging at 3T. AJNR Am J Neuroradiol. 2007; 28(3):433–438. [PubMed: 17353308]

194. Isoda H, Ohkura Y, Kosugi T, et al. *In vivo* hemodynamic analysis of intracranial aneurysms obtained by magnetic resonance fluid dynamics (MRFD) based on time-resolved three-dimensional phase-contrast MRI. Neuroradiology. 2010; 52(10):921–928. [PubMed: 20012431]

195. Hope TA, Hope MD, Purcell DD, et al. Evaluation of intracranial stenoses and aneurysms with accelerated 4D flow. Magn Reson Imaging. 2010; 28(1):41–46. [PubMed: 19577400]

196. Meckel S, Stalder AF, Santini F, et al. *In vivo* visualization and analysis of 3-D hemodynamics in cerebral aneurysms with flow-sensitized 4-D MR imaging at 3 T. Neuroradiology. 2008; 50(6): 473–484. [PubMed: 18350286]

197. Kecskemeti S, Johnson K, Wu Y, Mistretta C, Turski P, Wieben O. High resolution three-dimensional cine phase contrast MRI of small intracranial aneurysms using a stack of stars k-space trajectory. J Magn Reson Imaging. Mar; 2012 35(3):518–27. Epub 2011 Nov 16. DOI: 10.1002/jmri.23501 [PubMed: 22095652]

198. Schnell S, Ansari SA, Vakil P, et al. Three-dimensional hemodynamics in intracranial aneurysms: influence of size and morphology. J Magn Reson Imaging. 2014; 39(1):120–131. [PubMed: 24151067]

199. Grinstead JW, Sinha S, Tateshima S, Nien YL, Vinuela F. Visualization and quantification of flow and velocity fields in intracranial arteriovenous malformations using phase-contrast MR angiography. AJR Am J Roentgenol. 2006; 186(2):553–555. [PubMed: 16423967]

200. Wasserman BA, Lin WL, Tarr RW, Haacke EM, Muller E. Cerebral arteriovenous malformations — flow quantitation by means of 2-dimensional cardiac-gated phase-contrast MR-Imaging. Radiology. 1995; 194(3):681–686. [PubMed: 7862962]

201. Marks MP, Pelc NJ, Ross MR, Enzmann DR. Determination of cerebral blood-flow with a phase-contrast cine MR imaging technique — evaluation of normal subjects and patients with arteriovenous malformations. Radiology. 1992; 182(2):467–476. [PubMed: 1732966]

202. Alaraj A, Amin-Hanjani S, Shakur SF, et al. Quantitative assessment of changes in cerebral arteriovenous malformation hemodynamics after embolization. Stroke. 2015; 46(4):942–947. [PubMed: 25744522]

203. Chang W, Loecher MW, Wu Y, et al. Hemodynamic changes in patients with arteriovenous malformations assessed using high-resolution 3D radial phase-contrast MR angiography. AJNR Am J Neuroradiol. 2012; 33(8):1565–1572. [PubMed: 22499844]

204. Chang W, Wu Y, Johnson K, et al. Fast Contrast-enhanced 4D MRA and 4D flow MRI using constrained reconstruction (HYPRFlow): potential applications for brain arteriovenous malformations. AJNR Am J Neuroradiol. 2015; 36(6):1049–1055. [PubMed: 25698624]

205. Ansari SA, Schnell S, Carroll T, et al. Intracranial 4D flow MRI: toward individualized assessment of arteriovenous malformation hemodynamics and treatment-induced changes. AJNR Am J Neuroradiol. 2013; 34(10):1922–1928. [PubMed: 23639564]

206. Wu C, Ansari SA, Honarmand AR, et al. Evaluation of 4D vascular flow and tissue perfusion in cerebral arteriovenous malformations: influence of Spetzler–Martin grade, clinical presentation, and AVM risk factors. AJNR Am J Neuroradiol. 2015; 36(6):1142–1149. [PubMed: 25721076]

207. Amin-Hanjani S, Alaraj A, Calderon-Arnulphi M, Aletich VA, Thulborn KR, Charbel FT. Detection of intracranial in-stent restenosis using quantitative magnetic resonance angiography. Stroke. 2010; 41(11):2534–2538. [PubMed: 20930155]

208. Amin-Hanjani S, Rose-Finnell L, Richardson D, et al. Vertebrobasilar Flow Evaluation and Risk of Transient Ischaemic Attack and Stroke study (VERiTAS): rationale and design. Int J Stroke. 2010; 5(6):499–505. [PubMed: 21050408]

209. Baumgartner RW, Mattle HP, Schroth G. Assessment of >/=50% and <50% intracranial stenoses by transcranial color-coded duplex sonography. Stroke. 1999; 30(1):87–92. [PubMed: 9880394]

210. Wang L, Xing Y, Li Y, Han K, Chen J. Evaluation of flow velocity in unilateral middle cerebral artery stenosis by transcranial Doppler. Cell Biochem Biophys. 2014; 70(2):823–830. [PubMed: 24833432]

211. ElSankari S, Baledent O, van Pesch V, Sindic C, de Broqueville Q, Duprez T. Concomitant analysis of arterial, venous, and CSF flows using phase-contrast MRI: a quantitative comparison between MS patients and healthy controls. J Cereb Blood Flow Metab. 2013; 33(9):1314–1321. [PubMed: 23778162]

212. Gisolf J, van Lieshout JJ, van Heusden K, Pott F, Stok WJ, Karemaker JM. Human cerebral venous outflow pathway depends on posture and central venous pressure. J Physiol. 2004; 560(Pt 1):317–327. [PubMed: 15284348]

213. Stoquart-ElSankari S, Lehmann P, Villette A, et al. A phase-contrast MRI study of physiologic cerebral venous flow. J Cerebr Blood F Met. 2009; 29(6):1208–1215.

214. Stolz E, Kaps M, Dorndorf W. Assessment of intracranial venous hemodynamics in normal individuals and patients with cerebral venous thrombosis. Stroke. 1999; 30(1):70–75. [PubMed: 9880391]

215. Mehta NR, Jones L, Kraut MA, Melhem ER. Physiologic variations in dural venous sinus flow on phase-contrast MR imaging. AJR Am J Roentgenol. 2000; 175(1):221–225. [PubMed: 10882276]

216. Schuchardt F, Schroeder L, Anastasopoulos C, et al. *In vivo* analysis of physiological 3D blood flow of cerebral veins. Eur Radiol. 2015; 25(8):2371–2380. [PubMed: 25638218]

217. Hope MD, Purcell DD, Hope TA, et al. Complete intracranial arterial and venous blood flow evaluation with 4D flow MR imaging. AJNR Am J Neuroradiol. 2009; 30(2):362–366. [PubMed: 18653687]

218. Schrauben EM, Johnson KM, Huston J, et al. Reproducibility of cerebrospinal venous blood flow and vessel anatomy with the use of phase contrast—vastly undersampled isotropic projection reconstruction and contrast-enhanced MRA. Am J Neuroradiol. 2014; 35(5):999–1006. [PubMed: 24287088]

219. Nett EJ, Johnson KM, Frydrychowicz A, et al. Four-dimensional phase contrast MRI with accelerated dual velocity encoding. J Magn Reson Imaging. 2012

220. Ha H, Kim GB, Kweon J, et al. Multi-VENC acquisition of four-dimensional phase-contrast MRI to improve precision of velocity field measurement. Magn Reson Med. Jun 8.2015 [Epub ahead of print]. doi: 10.1002/mrm.25715

221. Callaghan FM, Kozor R, Sherrah AG, et al. Use of multi-velocity encoding 4D flow MRI to improve quantification of flow patterns in the aorta. J Magn Reson Imaging. Feb; 2016 43(2): 352–63. Epub 2015 Jun 30. DOI: 10.1002/jmri.24991 [PubMed: 26130421]

222. Johnson KM, Markl M. Improved SNR in phase contrast velocimetry with five-point balanced flow encoding. Magn Reson Med. 2010; 63(2):349–355. [PubMed: 20099326]

223. Nilsson A, Bloch KM, Carlsson M, Heiberg E, Stahlberg F. Variable velocity encoding in a three-dimensional, three-directional phase contrast sequence: evaluation in phantom and volunteers. J Magn Reson Imaging. 2012; 36(6):1450–1459. [PubMed: 23065951]

224. Schmitter S, DelaBarre L, Wu X, et al. Cardiac imaging at 7 Tesla: Single- and two-spoke radiofrequency pulse design with 16-channel parallel excitation. Magn Reson Med. 2013; 70(5): 1210–1219. [PubMed: 24038314]

225. van Ooij P, Zwanenburg JJ, Visser F, et al. Quantification and visualization of flow in the Circle of Willis: time-resolved three-dimensional phase contrast MRI at 7 T compared with 3 T. Magn Reson Med. 2013; 69(3):868–876. [PubMed: 22618854]

226. van Ooij P, Guedon A, Marquering HA, et al. k-t BLAST and SENSE accelerated time-resolved three-dimensional phase contrast MRI in an intracranial aneurysm. MAGMA. 2013; 26(3):261–270. [PubMed: 22955942]

227. Sekine T, Amano Y, Takagi R, Matsumura Y, Murai Y, Kumita S. Feasibility of 4D flow MR imaging of the brain with either Cartesian *y–z* radial sampling or k-t SENSE: comparison with 4D flow MR imaging using SENSE. Magn Reson Med Sci. 2014; 13(1):15–24. [PubMed: 24492737]

228. Kadbi, M.; Negahdar, M.; Traughber, M.; Martin, P.; Amini, AA. Assessment of flow and hemodynamics in the carotid artery using a reduced TE 4D flow spiral phase-contrast MRI. Annual International Conference of the IEEE Engineering in Medicine and Biology Society; 2013. p. 1100-1103.

229. Hutter J, Schmitt P, Saake M, et al. Multi-dimensional flow-preserving compressed sensing (MuFloCoS) for time-resolved velocity-encoded phase contrast MRI. IEEE Trans Med Imaging. 2015; 34(2):400–414. [PubMed: 25252278]

230. Tao YH, Rilling G, Davies M, Marshall I. Carotid blood flow measurement accelerated by compressed sensing: validation in healthy volunteers. Magn Reson Imaging. 2013; 31(9):1485–1491. [PubMed: 23830111]

231. Gatehouse PD, Rolf MP, Graves MJ, et al. Flow measurement by cardiovascular magnetic resonance: a multi-centre multi-vendor study of background phase offset errors that can compromise the accuracy of derived regurgitant or shunt flow measurements. J Cardiovasc Magn Reson. 2010; 12:5. [PubMed: 20074359]

232. Lorenz R, Bock J, Snyder J, Korvink JG, Jung BA, Markl M. Influence of eddy current, Maxwell and gradient field corrections on 3D flow visualization of 3D CINE PC-MRI data. Magn Reson Med. 2014; 72(1):33–40. [PubMed: 24006013]

233. Giese D, Haeberlin M, Barmet C, Pruessmann KP, Schaeffter T, Kozerke S. Analysis and correction of background velocity offsets in phase-contrast flow measurements using magnetic field monitoring. Magn Reson Med. 2012; 67(5):1294–1302. [PubMed: 21826731]

234. Busch J, Vannesjo SJ, Barmet C, Pruessmann KP, Kozerke S. Analysis of temperature dependence of background phase errors in phase-contrast cardiovascular magnetic resonance. J Cardiovasc Magn Reson. 2014; 16:97. [PubMed: 25497004]

235. Walker PG, Cranney GB, Scheidegger MB, Waseleski G, Pohost GM, Yoganathan AP. Semiautomated method for noise reduction and background phase error correction in MR phase velocity data. J Magn Reson Imaging. 1993; 3(3):521–530. [PubMed: 8324312]

236. Rigsby CK, Hilpipre N, McNeal GR, et al. Analysis of an automated background correction method for cardiovascular MR phase contrast imaging in children and young adults. Pediatr Radiol. 2014; 44(3):265–273. [PubMed: 24306733]

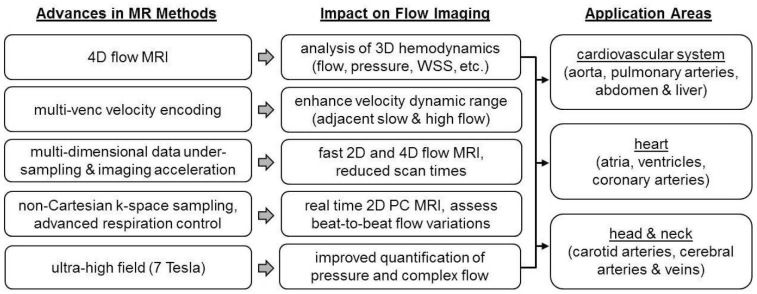

Fig. 1.

Summary of recent methodological advances, the impact on MRI flow imaging and quantification of haemodynamic parameters, along with their associated main applications.

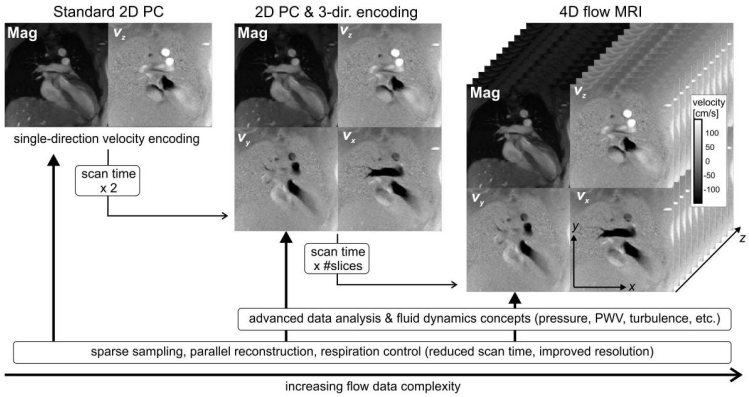

Fig. 2.

Chart illustrating the increased complexity and information content in flow data as a function of dimensionality and scan time. The role of methods development is shown along the bottom row, with an impact spanning standard 2D cine PC (left) to 4D flow MRI (right), with volumetric coverage and three-directional velocity encoding. Mag, magnitude image.

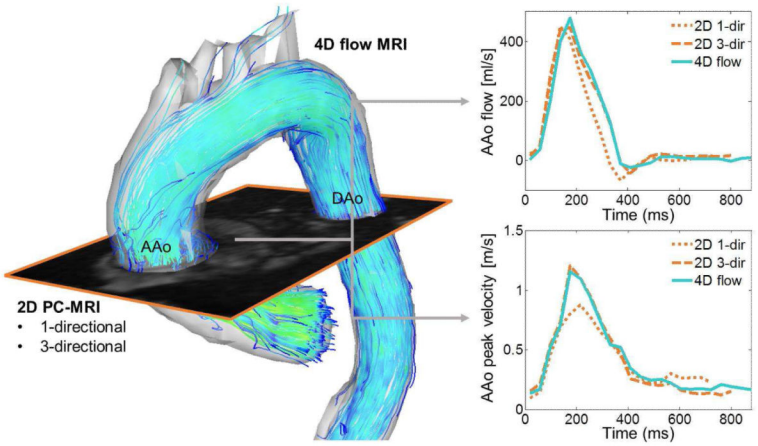

Fig. 3.

Comparisons of regional flow quantification in the ascending aorta (AAo) of a healthy subject by 4D flow MRI, 2D cine PC with three-directional velocity encoding (2D 3-dir), and standard 2D cine PC with one-directional through-plane velocity encoding (2D 1-dir). The imaging plane used for 2D CINE PC was co-registered with the 4D flow data to ensure flow unification at identical locations in the aorta. 3D streamlines (left) depict the systolic 3D velocity distribution and flow patterns in the thoracic aorta. The graphs (right) clearly show underestimation of systolic peak velocities by 2D 1-dir and close agreement between 4D flow and 2D 3-dir.

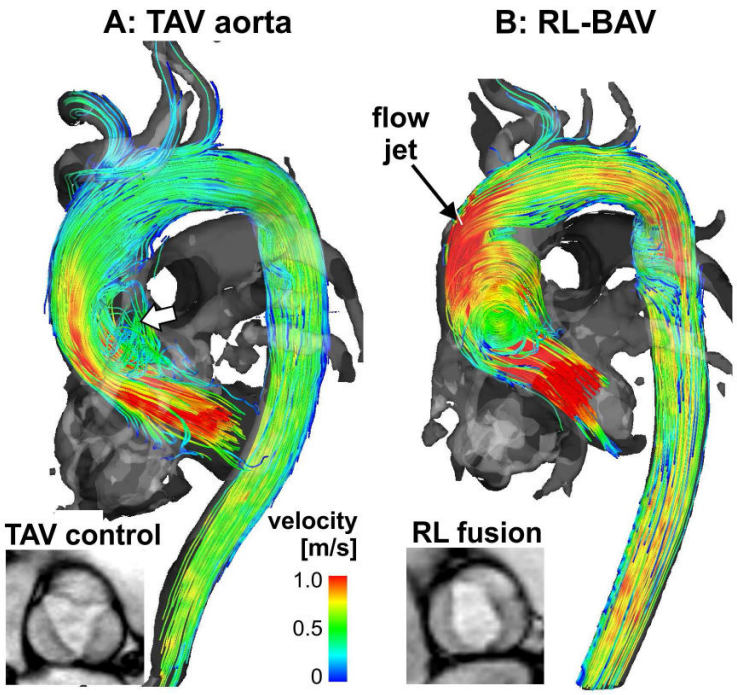

Fig. 4.

3D blood flow visualisation (systolic 3D streamlines) based on thoracic 4D flow MRI in a patient with a bicuspid aortic valve with a right–left fusion pattern (RL-BAV, b) compared to an aorta size-matched control subject with normal tri-leaflet aortic valve (TAV, a). Note that BAV resulted in a marked flow jet impinging on the aortic wall compared to TAV.

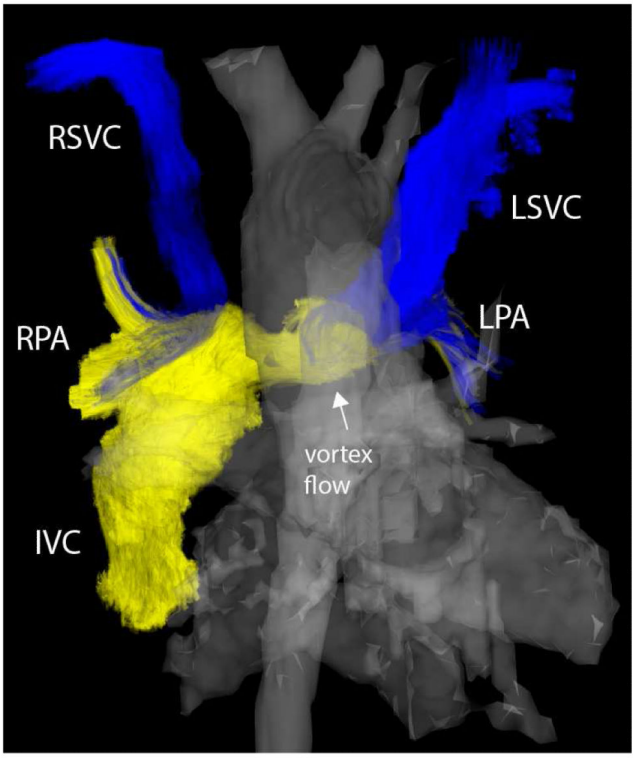

Fig. 5.

3D venous and arterial flow visualisation from 4D flow MRI for a patient with Fontan circulation. Venous return from the bilateral superior venae cavae (SVCs) and the inferior vena cava (IVC) flows to the right and left pulmonary arteries (RPA, LPA) by way of the Fontan connection, a surgically created vascular connection that directly routes venous return to the right and left lungs. Surrounding vessels of interest are shown in grey and include the aorta and pulmonary veins. Time-resolved path lines are colour-coded by vessel of origin: flow from the right and left SVCs (RSVC, LSVC) is shown in blue and flow from the IVC is shown in yellow. These results provide information regarding complex flow patterns and flow distribution, including the identification of vortex flow and the quantification of hepatic (or IVC) flow distribution to the RPA (88%) and LPA (12%).

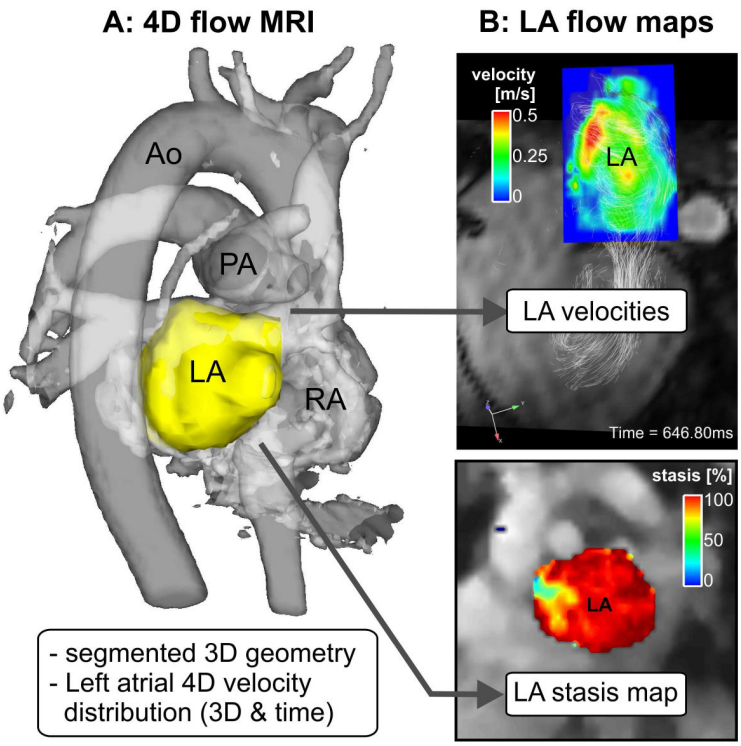

Fig. 6.

4D flow MRI and derived 3D PC angiogram (PC-MRA, a) including the 3D segmentation of the LA which was used to mask blood flow velocities inside the LA for the calculation of stasis (% of LA velocities <0.1 m/s) and velocity maps (b). Ao, aorta, PA, pulmonary artery, RA, right atrium.

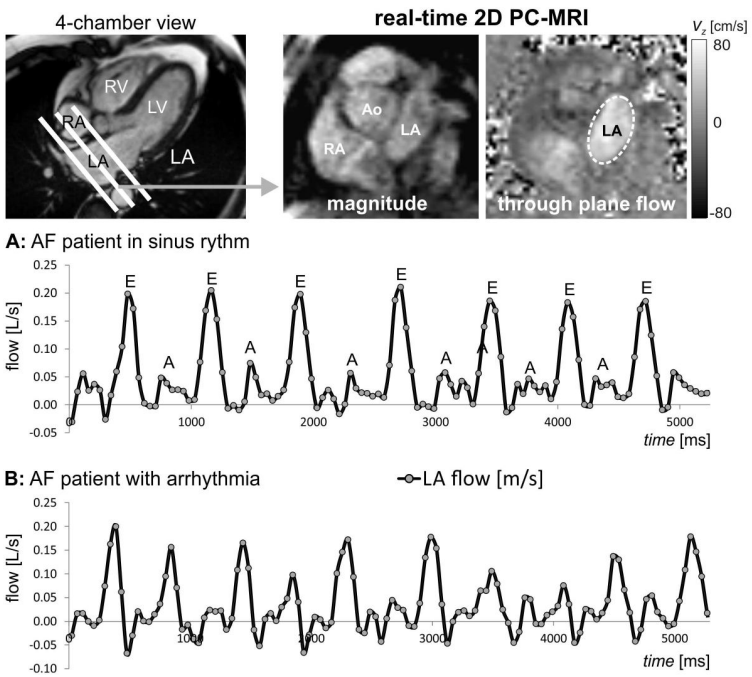

Fig. 7.

Real-time imaging of flow in the LA based on 2D PC with EPI data readout, shared velocity encoding, and spatiotemporal imaging acceleration (temporal resolution per image = 50 ms). Data were acquired without ECG gating and through-plane velocity encoding (total scan time=10 seconds, venc = 80 cm/s). Data analysis included the calculation of LA flow in region of interests delineating the LA boundary. Resulting flow-time curves at mid-atrial short axis level show flow changes over multiple heart beats in AF patients in sinus rhythm (a) and during arrhythmia (b).

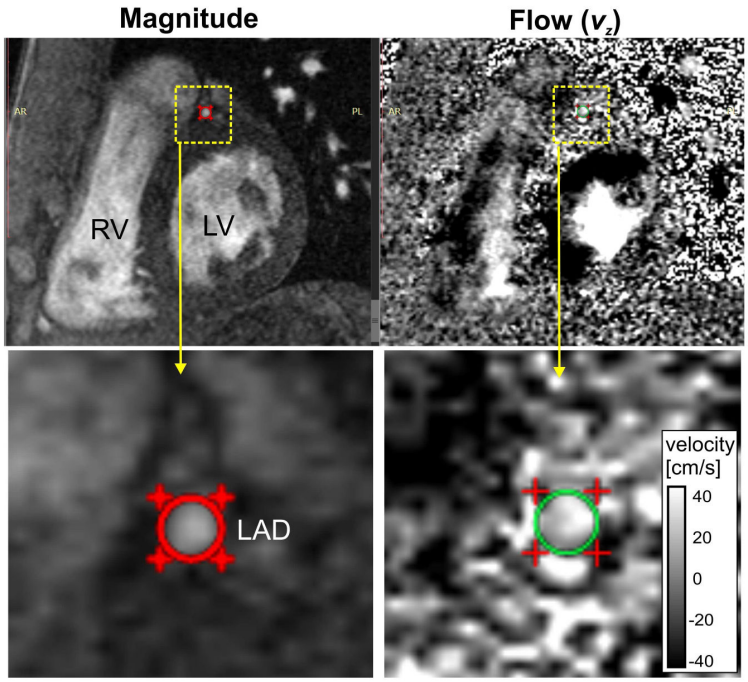

Fig. 8.

Coronary 2D PC MRI with through-plane velocity encoding. Data were acquired using k-t acceleration with a high acceleration factor of R=5 which allowed for data acquisition during a single breath hold and an in-plane spatial resolution of approximately 1 mm^2. The images show magnitude and flow data for peak coronary flow during early diastole. LV, left ventricle; RV, right ventricle; LAD, left anterior descending coronary artery.

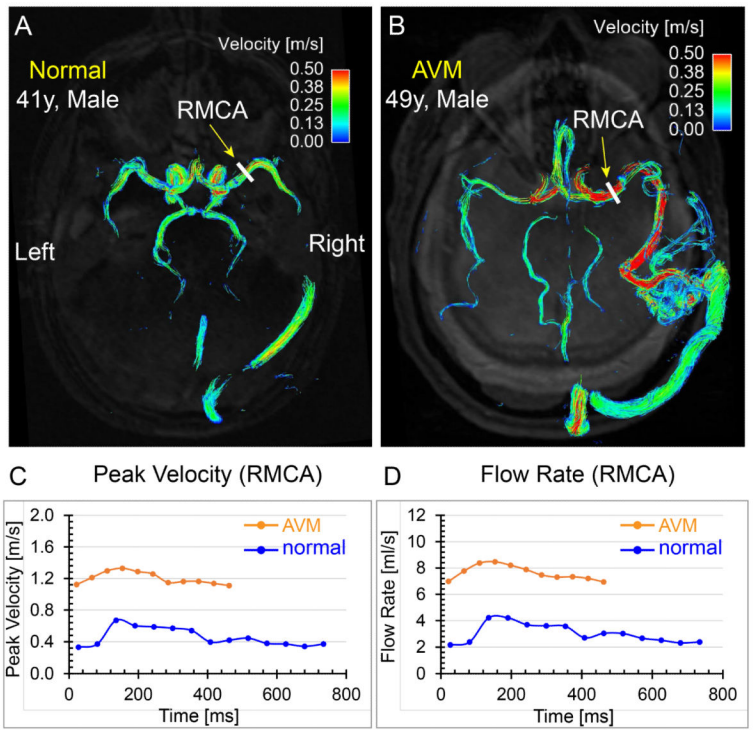

Fig. 9.

Comparisons of time-integrated 3D path lines and regional flow quantification between a 41-year-old male normal volunteer and a 49-year-old male patient with cerebral arteriovenous malformation (AVM). The path lines of the normal volunteer (a) show symmetric and coherent flow patterns in the cerebral arteries, whereas the path lines of the AVM patient (b) exhibit disturbed cerebral flow patterns and the velocity in the feeding right middle cerebral artery (RMCA) is much higher than the contralateral counterpart. The peak velocity (c) and flow-time (d) curves at the RMCA M1 segment (yellow arrows) quantitatively demonstrate higher blood flow and velocity in the AVM feeding artery compared to the same artery in the normal volunteer. Note that the average length of the cardiac cycle was shorter for the AVM patient compared to the normal volunteer during the scan.

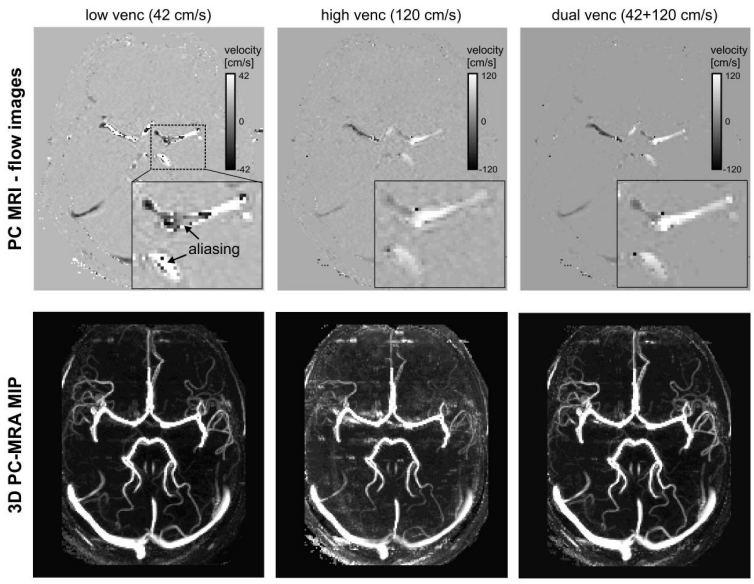

Fig. 10.

Intra-cranial dual-venc 4D flow MRI at 7 T (spatial resolution = 1.1 mm^3) for the assessment of cerebral vascular flow and angiography. Example flow images (top row) illustrate substantial velocity aliasing for the low venc data (left) but excellent velocity–background contrast and depiction of regions with low flow velocity. Conversely, velocity aliasing is absent in the high venc data (mid) but velocity background noise is increased and low flow regions are less well delineated. Dual-venc reconstruction of flow data (right) successfully removed velocity aliasing while maintaining the favourable dynamic range of the low venc data. Resulting 3D PCMRA maximum intensity projections (MIPs, lower row) of the entire 4D flow data corroborate these findings. The depiction of the cerebral vasculature (especially small arteries and veins with slow flow) is considerably improved for the dual-venc reconstruction (right). Data were acquired at UM CMRR (Minneapolis) using an actively shielded 7 T system with high-performance gradients (G_{max} 72 mT/m, slew rate 200 mT/m/ms) and a 32-channel head coil.